P-64

Lunar and Planetary Science XXI

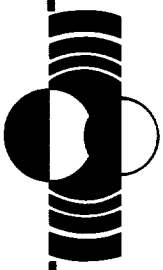

Abstracts of papers submitted to the Twenty-First Lunar and Planetary Science Conference

PRESS ABSTRACTS

NASA

National Aeronautics and Space Administration

Lyndon B. Johnson Space Center
Houston, Texas

LPI / USRA

LUNAR AND PLANETARY INSTITUTE
UNIVERSITIES SPACE RESEARCH ASSOCIATION

PRESS ABSTRACTS

TWENTY-FIRST LUNAR AND PLANETARY SCIENCE CONFERENCE

March 12-16, 1990

Compiled by the
Lunar and Planetary Institute
3303 NASA Road 1
Houston, Texas 77058-4399

LPI Contribution 740

Business Telephone Numbers of First Authors

T. J. Ahrens (correspondence author) 818-356-6905

V. R. Baker 602-621-6003

J.-P. Bibring 33-1-69415256

R. N. Clayton 312-702-7777

J. S. Delaney 201-932-3636

T. Graf 619-534-0443

B. B. Holmberg 617-495-7299

R. L. Kirk 602-527-7181

T. J. McCoy 505-277-5444

W. B. McKinnon 314-889-5604

V. R. Oberbeck 415-694-5496

S. Saunders 818-393-1001

P. H. Schultz 401-863-2417

E. M. Shoemaker 602-527-7181

J. R. Spencer 808-948-8138

S. K. Stephens 818-356-6961

M. K. Zolensky (correspondence author) 713-483-5128

PREFACE

The Program Committee for the Twenty-first Lunar and Planetary Science Conference has chosen these contributions as having the greatest potential interest for the general public. The papers in this collection have been written for general presentation, avoiding jargon and unnecessarily complex terms. More technical abstracts will be found in *Lunar and Planetary Science XXI.*

For assistance during the conference, call the NASA Johnson Space Center News Center at 713-483-5111. Telephone numbers of the first author of each contribution will be found on page iii. Feel free to call for more information.

CONTENTS

Ancient Ocean-Land-Atmosphere Interactions on Mars: Global Model and Geological Evidence

by

Victor R. Baker, Robert G. Strom, Steven K. Croft,
Virginia C. Gulick, Jeffrey S. Kargel, and Goro Komatsu
Department of Planetary Sciences
Lunar and Planetary Laboratory
University of Arizona
Tucson, Arizona 85721

An Exciting Discovery

Discoveries in science include both new information about nature and new ways of understanding the information already in hand. We report here on a new understanding of global environmental change on Mars achieved from study of existing data. This new view of climatic change on Mars struck us in late December as we pondered a great variety of perplexing surface features on the planet.

For many years, like other planetary geologists, we were puzzled by numerous enigmas on Mars. Why did some portions of the surface seem to have very low erosion rates, while other areas have forms indicating intense degradation by erosional processes? Why did numerous valleys and channels form during the Martian past, when the modern climate is too cold and dry for active water flow? How could water have moved to replenish ancient streams when the modern atmosphere has less than 1/100 the pressure of that on Earth?

The answer to these and other Martian dilemmas is provided by temporary past episodes of ocean formation. We find that vast areas of the northern lowland plains on this dry, desert planet were sporadically inundated by huge quantities of water. Repeated formation and dissipation of this ocean, which we name Oceanus Borealis, resulted in relatively warm, wet climatic epochs that favored the development of glaciers in the southern hemisphere and highlands of Mars. Rainfall and surface-water flow in valleys were dominant early in the planet's history. Lake formation, melting of permafrost, active landsliding, and erosion of old craters all seem to have occurred during the temporary warm, wet (maritime) mode of Martian climate. When the oceans gradually evaporated or froze, the planet returned to its cold, dry condition with its water trapped as ground ice in underground permafrost. It is this cold, dry mode which presently characterizes Mars.

The last formation of Oceanus Borealis came relatively late in Martian history. Sediments deposited by this ocean had been described by several investigators prior to our work. The oceanic evidence was most impressively assembled by T. J. Parker, R. S. Saunders, and D. M. Schneeberger of the Jet Propulsion Laboratory, California Institute of Technology. Stimulated by their work and by a vast array of studies by many planetary geologists, we developed the following global model of ocean formation on Mars.

Mars Climate Model

Models are theoretical simplifications of how scientists perceive the operation of phenomena. Our model arose intuitively from experience with Martian phenomena and from hypothesizing the origin and consequences of an ocean.

During later Martian history huge concentrations of molten rock (magma) were concentrated at one local region of the planet, the Tharsis volcano area. Massive and rapid emplacement of magma beneath this bulging hot spot melted huge amounts of ground ice, driving it into fractures on the margins of the Tharsis bulge. The water burst on to the surface at great outflow channels heading at these fractures. Driven by volcanic heat, the cataclysmic outburst floods of water and mud carved immense, spectacular channels, tens of miles wide. The warm water inundated the northern plains of Mars, vaporizing the north polar cap of carbon dioxide ice.

The cataclysmic ocean formation had an immediate climatic influence. Both water (evaporated from the sea) and carbon dioxide (from the polar cap) are greenhouse gases. Just as human burning of fossil fuels is causing a global warming of Earth, so the Martian floods induced a cataclysmic warming. As Martian temperatures rose, other water, frozen in upland permafrost, was released to flow into lakes or the Oceanus Borealis. The climate moved to its maritime state, with precipitation possible.

During the late phase of ocean formation, much of the precipitation fell as snow. Particularly near the south pole and in upland areas, the snow accumulated to thicknesses sufficient to form ice. As the snow and ice built up, it flowed as glaciers. The geological evidence indicates that the glaciers advanced and retreated, much the same as occurred in the Ice Ages of Earth. Because the late Mars ocean was relatively short-lived, this Martian glacial epoch was also very brief.

Oceanus Borealis was probably a persistent feature early in Mars history. At that time the planet was experiencing a relatively high rate of impacting objects. The dense water and carbon

dioxide atmosphere allowed precipitation as rain, resulting in the widespread valley networks of the Martian uplands. However, water was being lost because of dissociation in the upper atmosphere of the planet. The hydrogen was lost to space while the oxygen contributed to the red color of the planet by oxidizing various materials. Eventually water loss and precipitation of the carbon dioxide as carbonate rock reduced the atmospheric pressure below the greenhouse level for maintaining the ocean. Most of the water was sequestered into the very permeable rocks of the planet where it comprised ice in a permafrost.

The ocean was able to reform much later in the planet's history because of the Tharsis volcanism described above. This cataclysmic ocean was smaller than the original because of the water loss by hydrogen escape. However, it was big enough to temporarily modify the climate, producing the enigmas that had bothered us about the Martian surface.

Importance

The above model has completely changed how we view Mars. Instead of a cold, dry world with enigmatic features inconsistent with its modern climate, we now see a more earthlike planet. During its early history Mars was very water-rich, and it seems to have had a watery atmosphere. Unlike Earth, the rocks and landscapes of Mars' first billion years of history are well preserved. Did life form in the early Martian ocean? If so, fossils of that life might be present and available for discovery by a future geological exploratory mission. On Earth we have little or no material left from that early period because of the active reworking of the planet's surface. The stable Martian surface is a unique record of the same watery past that characterized our own planet.

Mars and Earth are the only known planets on which water has moved in a dynamic cycle from its reservoir in the ocean to rainfall, flowing rivers, and back to the sea. This same cycle, the hydrological cycle, is the source and the maintainer of life on Earth. Might it have served as the source for life on Mars as well? We may find the answer to the origin of life on Mars rather than on Earth.

Science Issues

Sometimes science is viewed as a monolithic enterprise of computers, laboratory equipment, and individual theorists. We forget that science is a group exercise in which people make sense, a kind of common sense, out of the world in which they live.

We feel we have found a way to make sense out of what seemed to be perplexing problems of past environmental change on the planet Mars. The way that this has changed our view gives hope that a similar sense can be achieved about the perplexing problems of future environmental change on the planet Earth. Is there something in the existing information that we are just not seeing? Can one simple idea give us the clue to how it all fits into a pattern?

We have a new confidence on how Mars works as a planet, how its water-related systems have evolved through time. We need a similar confidence for Earth. Rather than idealized future "scenarios" given to us by computers, we need an understanding of how the whole planet works. If we can figure it out for a slightly smaller, slightly colder version of Earth known as Mars, that process of common sense should allow us the same revelation about Earth and its global changes. As the philosopher William Clifford once said of science, ". . . the truth at which it arrives is not that which we can ideally contemplate without error, but that which we may act upon without fear."

THE OBSERVATION OF MARS BY THE ISM INSTRUMENT ON BOARD THE PHOBOS 2 SPACECRAFT;

J-P Bibring, Y. Langevin, S. Erard, B. Gondet, O. Forni, P. Masson, C. Sotin and A. Soufflot, *Institut d'Astrophysique Spatiale, 91405 Orsay, France*; M. Combes, P. Drossart, T. Encrenaz, E. Lellouch and J. Rosenqvist, *DESPA, Observatoire de Meudon, France*; V.I. Moroz, N. Sanko, A.V. Grigoryef and Y.V. Nikolsky, *IKI, Moscow, USSR*

Abstract

ISM is a near-infrared imaging spectrometer, that operated on board the soviet Phobos 2 spacecraft. It acquired 40,000 spectral images of Mars, with a spatial resolution ranging from 5 to 30 km. It also observed Phobos two times, from a distance of 200 km: the achieved resolution is .7 km. ISM detected signatures of the major atmospheric and mineralogic constituents. Concerning the surface, the major result is the high level of its heterogeneity, on a scale close to the ISM resolution, observed for all properties: albedo, colour, composition, degree of hydration of the soil.

Introduction

The Soviet Phobos 2 spacecraft remained in orbit around Mars from early February up to March 25, 1989. The minimum distance from the surface of Mars was less than 900 km during the first elliptical orbits, and 6300 km from the circular orbits. At the very end of the mission, the spacecraft was tilted in order to point Phobos, the largest martian moon, from a distance close to 200 km.

Our instrument, named ISM (Infrared SpectroMeter), is an infrared imaging spectrometer operating from .8 to 3.2 micrometers (1,2). This instrument, entirely conceived and manufactured in France, constitutes the first ever flown imaging spectrometer for planetary observations. It consists in a telescope 2.5 cm in diameter, providing a 12 arcmin field of view. Converted into spatial resolution, the pixel size ranges from 5 to 30 km on Mars, depending on the altitude of the spacecraft, and 0.7 km on Phobos. The imaging capability was provided in the crosstrack direction by a scanning mirror, moving by steps ±20° away from the optical axis, and downtrack by the motion of the spacecraft. As the orbit of the spacecraft was equatorial, ISM was restricted to areas with latitude lower than 30°.

The spectroscopic range was obtained with a grating used in the first and second orders, separately focused onto two 64-pixel PbS arrays. The

detector operational temperature was provided by means of a passive cooling down to 200 K, monitored to 0.1 K. The signal/noise ratios achieved were remarkable, higher than 1000 for typical integration times of one second, over most of the spectral range.

The data set

ISM was first turned on two times from a low altitude, which provided two high resolution tracks, 20 km large and 1650 km long. They both are located close to the equator in the Tharsis region, crossing Pavonis Mons, one of the main martian volcanoes. Most of the observations were then performed from the circular orbit, when the spacecraft was three-axis stabilized. Each image maps an area 400 x 3000 km^2 typically. Seven of them are located in the western hemisphere: most of Valles Marineris and all Tharsis volcanoes are thus mapped, at least partially, including Olympus Mons, the highest one (more than 25,000 meters in altitude). In the eastern hemisphere, the old cratered terrains of Arabia Terra, as well as Isidis Planitia and Syrtis Major, have also been imaged. Altogether, ISM has sampled most major geological units, with the noticeable exception of the polar caps, that could not been observed from the equatorial orbit.

On Mars 25, when the spacecraft pointed Phobos, ISM was turned on two times. For the first observation, ISM acquired a track one pixel large across more than half of the lighted Phobos hemisphere, close to its equator. During the second observation, ISM mapped an area 20 x 20 km^2, constituted of more than 400 contiguous pixels. This infrared image constitutes the first ever made of a solar system "small body": Phobos is considered as a C-type asteroid captured by Mars. Results on Phobos are presented elsewhere (3).

Results on the martian atmosphere

Although the spectral resolution of ISM was not designed to resolve the individual lines of gazeous species, the martian spectra exhibit the enveloppes of the features associated to the main bands of CO_2, by far the major atmospheric constituent, as well as CO and H_2O bands. Through the CO_2 band, we measure the *total pressure*. Consequently, its variation from one pixel to the other is directly linked to the variation in *altimetry*. ISM has thus the capability of providing altimetric maps, with a vertical resolution of a few hundred meters. The CO/CO_2 ratioes have been measured, in all

regions where high volcanoes are located: along their slopes the total pressure varies, which allows to monitor the CO relative abundance when the CO_2 varies.

Our data do not fit with those obtained from the ground, with a much lower resolution. It is difficult to account for our data with a ratio constant with altitude, except if we assume a very low value, close to 10^{-4}, which is at least 5 times lower than observed from the Earth. If we take a value at zero altitude matching the one deduced from ground-based observations, a large CO depletion at high altitude is derived from our data. It might originate from heterogeneous chemistry, likely to play a role in catylizing the CO + O reaction onto aerosols. The H_2O/CO_2 ratio has also been measured. It appears constant, at a value close to 10^{-4}, within the experimental uncertainties.

Results on the martian surface

The near-infrared spectra of Mars originate mainly from the diffusion by the martian surface of the solar light. Two types of results can thus be inferred. First, the intensity of the diffused light give a measurement of the *brightness* of the surface (or its *albedo*), directly linked to global surface properties. In addition, the presence of surface minerals which absorb infrared radiation at given wavelengths give rise to absorption features whose spectral position and intensities can be used to infer the surface *mineralogy*, after appropriate laboratory simulations.

The infrared brightness of Mars appears to vary by very large factors from place to place. For example, Isidis Planitia is about three times darker than the surrounding plain. Similar contrasts are present between the canyon and the plateau of Valles Marineris. In addition to these variations on a large scale, small scale variations, on a kilometric scale, are clearly detected in our images. They all originate from differences in surface composition. As a general trend, dust deposits seem to be brighter, which enables to map their surface distributions, as well as their variation with time.

It is clear that numerous regions are not covered by dust of uniform composition. Large variations from one pixel to the other are present, in particular in the spectral features corresponding to the main silicate content and to the degree of hydration of the surface. The latter index is of particular interest, as it is linked to the general problem of the water cycle on Mars. Was liquid water stable, which would mean that the atmosphere was dense enough to allow the partial pressure of water and its temperature to be sufficiently high ? Are the ferric-rich minerals, responsible for the red

colour of the soil, originating from their oxydization by water ? Do the channels result from large flows of running water ? Are there sites where, within the water, chemical reactions proceeded, leading to evolved organic molecules ? Such questions can be partially answered by mapping the hydration spectral band over Mars. ISM data show that all spectra exhibit an intense band centered at 2.7 micrometers, that we attribute to water molecules or OH radicals blocked within the matrices of the surface soils. This indicates that hydration took place in the past. Furthermore, the intensity of this feature varies spatially by large amounts, indicating that the degree of hydration is not uniformely distributed over the martian surface. In particular, there is a general trend of increase of hydration along the slopes of the volcanoes. It might be the indication of hydration originating from the volcanic activity, the magma being processed by the underlying permafrost-rich layers before floading out of the volcanoes.

Future of ISM data reduction

The entire data set has been given to a number of selected groups in the United States, in Italy and in DDR. Consequently, not only French and Soviet Institutes are involved in the analyses. We have open our experiment to cooperation with scientists from USGS at Flagstaff, from Brown University at Providence, from Hawaï University at Honolulu and from Ames Research Center at Moffett Field, from Frascati and Roma, as well as from East Berlin. It should improve the scientific return of this pioneering experiment, which prepares the future exploration of Mars, by the OMEGA/VIMS experiment on board the soviet Mars 94 mission, of the Saturnian system, by the VIMS instrument on the CASSINI (NASA/ESA) orbiter, and the nucleus of comet P/Koppf, which will be mapped by VIMS/CRAF.(NASA).

References

(1)Bibring et al., *Nature, 341, 6243, 591-592*, 1989.
(2) Bibring et al., *Proceedings of 20th LPSC*, 1990.
(3) Langevin et al., *Lunar Planet. XXI*, LPI,Houston,1990

OXYGEN ISOTOPIC COMPOSITIONS OF ORDINARY CHONDRITES AND THEIR CHONDRULES; Robert N. Clayton[1,2], Toshiko K. Mayeda[1], Edward J. Olsen[3], and J.N. Goswami[4]. [1]Enrico Fermi Institute, [2]Departments of Chemistry and of the Geophysical Sciences, University of Chicago, Chicago, IL 60637; [3]Field Museum of Natural History, Chicago, IL 60605; [4]Physical Research Laboratory, Ahmedabad 380 009, India.

The oxygen isotopic compositions of chondrites and their internal constituents (chondrules, inclusions, xenoliths, matrix, etc.) are highly variable, and, in general, do not follow mass-dependent fractionation patterns. They serve, therefore, as tracers of reservoir-reservoir interactions in the solar nebula, and thus can be used to study the formation of chondrules and the processes by which they are assembled into chondrites. Several regularities are well established: (1) three isotopically distinct chondrule reservoirs exist, corresponding to ordinary, carbonaceous, and enstatite chondrites; (2) the reservoir of carbonaceous chondrite chondrules is common to all sub-classes of carbonaceous chondrites; (3) the reservoir of ordinary chondrite chondrules is common to all iron-groups of ordinary chondrites; (4) whole-rock isotopic compositions of equilibrated H, L, and LL chondrites are different, and follow an ^{16}O-mixing trend.

In the interpretation of the oxygen isotope data, several major problems remain unsolved: (1) do the separate reservoirs for ordinary, carbonaceous, and enstatite chondrites represent major spatial or temporal heterogeneities in the solar nebula? (2) What are the implications of isotopic mixing lines for chondrule formation? (3) How are the H, L, LL whole-rock isotopic compositions established? (4) What is the nature of UOC matrix? (5) What is the genetic relation of UOC to EOC?

Fig. 1 shows whole-rock isotopic data for 68 EOC falls. The three iron groups are resolved, and their means define a slope-1 mixing line referred to as the Equilibrated Chondrite Line (ECL). Fig. 2 shows isotopic data for 65 individual chondrules from ordinary chondrites (OC) and 53 chondrules from carbonaceous chondrites (CC). ECL is shown for reference; CCC is a least-squares fit to the CC chondrule data, and is almost coincident with the CAI mixing line. The combined CAI-CCC line extends over a range of almost 50‰, and very likely represents interaction between an ^{16}O-rich solid end-member near –40‰ and an ^{16}O-poor nebular gas reservoir which lies near the extrapolation of the mixing line toward the upper right. In contrast, the ordinary chondrite chondrule data span only about 5‰, for a similar total number of samples. It is very difficult to construct a simple two-component mixing model which gives such a limited spread of data. This is especially so when the range in $\delta^{18}O$ is comparable to the magnitude of the *equilibrium* gas-solid fractionation factor. The problem is illustrated in Fig. 3, which shows schematically the consequences of gas-solid exchange under such conditions. Point *G* is taken as the isotopic composition of an infinitely large gas reservoir. Point *E* is the composition of solids in equilibrium with the gas at *G*. Points *S1*, *S2*, *S3* represent the compositions of various solids before exchange, assumed to lie on an ^{16}O mixing line through *G*. The lines *S1–E*, *S2–E*, *S3–E* show the trajectories followed in gas-solid exchange reactions, and illustrate the expected spread of data for a set of incompletely equilibrated samples. The graph shows that short mixing lines generated in this way do not have slopes near unity. In fact, short slope-one mixing lines can only be formed by a special choice of compositions of starting materials. However, it can be shown that an array such as that observed for ordinary chondrite chondrules can be formed by a series of exchange events; i.e. multiple accretion and melting processes for each chondrule. The distinction between CC chondrules and the OC chondrules is that the former have undergone much less processing by multiple melting than the latter.

The OC chondrule data of Fig. 2 present a problem in understanding the whole-rock isotopic composition of H-chondrites. Almost all the single chondrules have oxygen which is isotopically heavier than mean H-chondrites. Material balance in H-chondrites is achieved only by inclusion of ^{16}O-rich chondrules and fragments <250 μm in diameter. Fig. 4 shows the data on size-fractions of Dhajala (H 3.8). Since H-chondrites contain a larger proportion of small chondrules than L- and LL-chondrites, it is likely that the distinctive isotopic compositions of the three iron groups are a consequence of a size-sorting of chondrules and fragments during accretion, with chondrules for all OC being derived from a common pool.

OXYGEN ISOTOPES IN CHONDRITES: Clayton R.N. et al.

Isotopically distinctive matrix material has been sought in several OC. None has been found, with the possible exception of ALH 77299, which contains "matrix lumps" which are isotopically light [1]. It has not yet been shown with certainty that this material is not disturbed by Antarctic weathering.

Some UOC have whole-rock isotopic compositions which are within the range of EOC for the same iron-group, especially H3 and L3 chondrites. LL3 chondrites, on the other hand, are all heavy-isotope enriched, extending to the right of the ECL by up to 2‰. Some of this effect might be due to aqueous alteration on the parent body, as has been observed in Semarkona [2]. Neither chondrules [3] nor matrix [4] in LL3 show the systematic effects evident in the whole-rocks. Some component not yet sampled must cause the isotopic shift. Its future identification may resolve the genetic relationships between UOC and EOC.

References: [1] G.C.A. **53**, 2081 (1989); [2] E.P.S.L. **95**, 187 (1989); [3] E.P.S.L. **65**, 209 (1983); [4] Meteoritics **22**, 395 (1987).

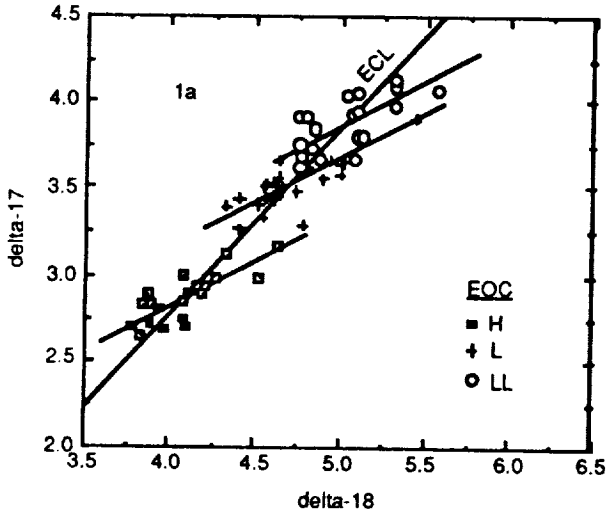

Fig. 1

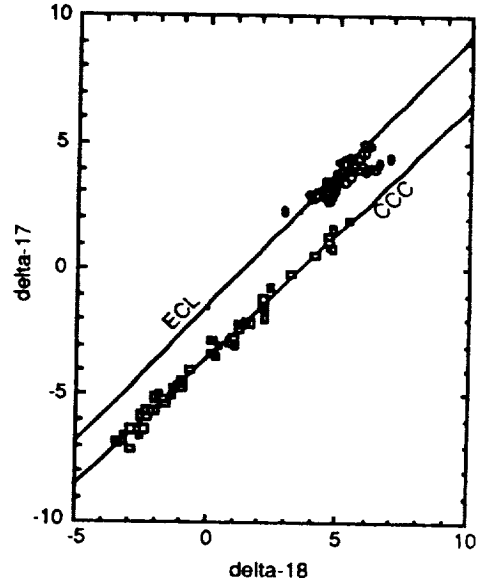

Fig. 2

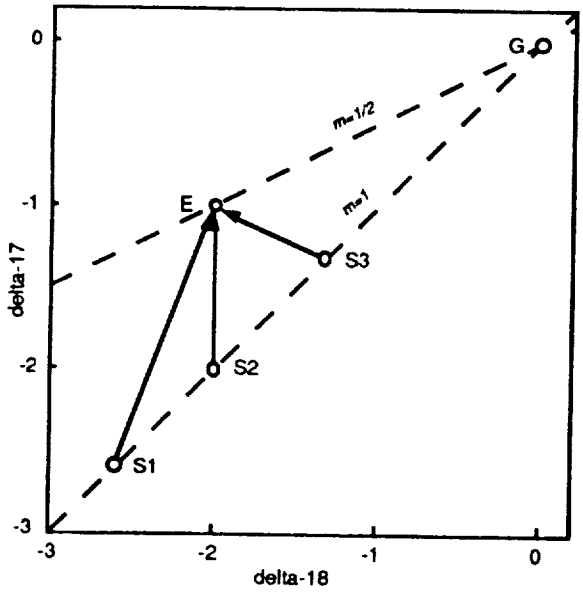

Fig. 3

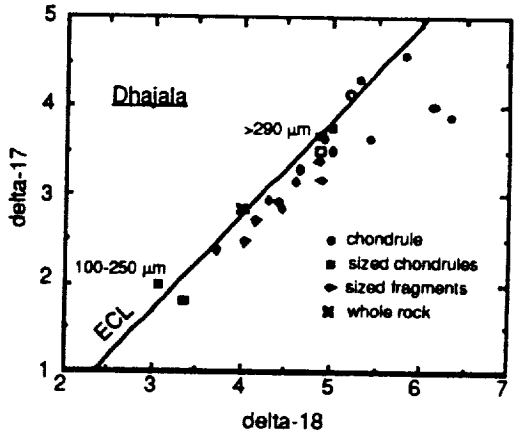

Fig. 4

LUNAR MARE BASALT FOUND AS METEORITE FROM ANTARCTICA

JEREMY S. DELANEY
Department of Geological Sciences, Rutgers University, New Brunswick, NJ 08903
Tel. 201/932-3616 FAX 201/932-5312

PAUL H. WARREN
Institute of Geophysics and Planetary Physics, University of California, Los Angeles, CA 90024-1567
Tel. 213/825-2015 FAX 213/206-3051

Meteorite collecting expeditions to the Elephant Moraine region of Antarctica have recovered a sample of the lunar maria. The recovery of this meteorite, rich in mare basalt material, is a major find. Several lunar meteorites have been collected in Antarctica since 1979, but all the previously identified finds are from the heavily-cratered, aluminum-rich highlands terrain that constitutes most of the lunar crust. The maria are dark, iron-rich volcanic formations, roughly analogous to the dominant type of rock in the oceanic crust of the Earth. *Maria* is the plural form of *mare*; this adaptation from Latin originated with Galileo, who noted a topographical resemblance to the Earth's *seas*. Maria are relatively abundant on the Moon's nearside hemisphere, which always faces the Earth, but they cover only 1/6 of the total lunar surface. Indeed, by most estimates the maria represent less than 1% of the total volume of the lunar crust. They appear to be very thin veneers of volcanic rock (basalt) covering parts of the older light colored highlands (anorthosite) crust. Mare basalts are generally young, by lunar standards (which is actually extremely ancient: 3 to 4 billion years old), and they tend to fill the enormous basins formed by giant meteorite impacts on the surface of the moon about four billion years ago. The lunar highlands, which make up the bulk of the lunar crust, formed in the first half billion years of planetary history.

The Elephant Moraine sample is a "breccia": i.e. a rock made up of numerous broken fragments of basaltic rock set in a matrix of smaller broken mineral grains and glassy material. These breccias are created by meteorite impacts on the surface of the Moon. Examination of the fragments and of the bulk rock itself reveals that the sample is a type of mare basalt called a very- low-titanium (VLT) basalt. This type of basalt contains very small amounts of the titanium bearing minerals that are both characteristic and abundant in many of the mare basalts returned by the Apollo missions. Both the lithic clasts and the matrix material around them contain the same suite of minerals: olivine, pyroxene and feldspar are dominant and several other minerals appear as minor proportions. The dark fraction (pyroxene and olivine) is the most abundant and its predominance distinguishes this sample from the lunar highlands rocks which are dominated by the light colored feldspar minerals. Lunar pyroxene and olivine are both magnesium-iron silicate minerals, whereas lunar feldspar is a calcium-aluminum silicate mineral. Detailed examination of the minerals in the Elephant Moraine meteorite reveal a range of compositions that is typical of the VLT basalts, with only small amounts of material from other sources. It is probable, therefore, that despite the disruption involved when the impact events on the surface of the Moon turned the original mare basalt into a breccia, that the breccia was assembled mostly from locally derived material. Comparison with the Apollo and Luna collections reveals that

small amounts of very-low-titanium basalt were brought back from the Moon only by the Apollo 17 and Luna 24 missions. The 30.7 gram (about 1.1 ounce) sample recovered at Elephant Moraine is, therefore, a large fraction of the total available VLT basalts on Earth. Remote sensing data acquired from lunar orbit suggests that VLT basalts fill a significant fraction of the lunar mare basins and that they are poorly represented by the returned samples from the Moon.

The precise area on the surface of the Moon from which the Elephant Moraine mare basalt breccia was ejected is unknown and there is presently no evidence available to identify its source. Unlike the earlier meteorite discoveries that sample lunar highlands material almost exclusively and, as a result, might be derived from almost anywhere on the surface of the Moon, the very specialized chemical features of this Elephant Moraine meteorite suggest that it is derived from one of several chemically distinct regions on the lunar nearside that can be recognized in the orbital mapping data. The largest VLT basins are in the northern hemisphere but without sample return missions to these maria, identifying the exact source region of the Elephant Moraine meteorite will probably not be feasible. Of the previous sample return missions to the Moon only Luna 24 landed in a mare basin that appears to have very low or low titanium basalts on the basis of remote sensing data.

Another lunar meteorite, discovered only a few months ago in the MacAlpine Hills region of Antarctica, has also been studied for the first time. It is the largest lunar meteorite yet discovered (comprising two stones with a total mass of 744 grams, or about 1.6 pounds). It has a mineralogy, texture, and composition indicative of derivation from a lunar highlands region, much like the source regions of the several lunar meteorites that had previously been analyzed. These lunar highlands meteorites are generally similar to the highlands samples acquired on the Apollo 16 mission (1972). One difference is that the lunar highlands meteorites analyzed to date have consistently had far lower concentrations of uranium and other elements that tend to correlate with uranium (e.g., thorium, rare earth elements). This difference is important, because uranium and thorium are the main sources of heat inside the Moon, and because some theories for the origin of the Moon and the Earth predict relatively high uranium (and thorium, etc.) for the Moon.

Lunar meteorites are usually easy to distinguish from other types of meteorites. No other type of meteorite is nearly so feldspar-rich as a typical lunar highalnds sample. However, the Elephant Moraine mare basalt meteorite is superficially similar to another, more common type of iron-rich basaltic meteorite known as eucrites. The Elephant Moraine sample was originally assumed to be a eucrite (eucrites are probably derived from disrupted asteroids), until our analyses of several geochemical ratios revealed traits (such as a relatively high iron/manganese ratio, and relatively low sodium/calcium and gallium/aluminum ratios) that only a lunar rock, and certainly not a eucrite, could possess. Very definite confirmation that both the Elephant Moraine and the MacAlpine Hills meteorites are lunar has been supplied in the form of data for the proportions of the three common isotopes of oxygen (reported by R. N. Clayton and T. K. Mayeda, of the University of Chicago). The proportions of the oxygen isotopes vary from planet to planet, but remain relatively fixed throughout all of the material within any large planet, and thus their measurement can yield powerful constraints on possible provenance of meteorites.

Lunar meteorite samples from Antarctica have been collected by American expeditions, sponsored by the National Science Foundation (with some support from NASA), and by

Japanese expeditions, organized by the National Institute of Polar Research. Since 1982, when the first lunar meteorite was identified as such, the number of known lunar meteorites has increased slowly but steadily. The total count of lunar meteorites, all from Antarctica, is now up to 10. However, when cases of evident "pairing" are eliminated (many meteorites break apart either during passage through the Earth's atmosphere or upon impact with the Earth's surface), the tally drops to 7.

These samples have revealed many surprises and insights. Until the discovery of the mare basalt at Elephant Moraine and another sample from the Japanese collections that is being reported at this meeting, only lunar highlands samples had been recognized. With the recognition of these mare basalts it is clear that we are getting samples of the Moon from a much wider spread of localities than were available from the previous sample return missions. These random samples from the Moon, therefore, provide independent tests for models of lunar history based on the sample return missions of the 1969-1976 period. For technological reasons, the landing sites of those missions were clustered within a small region of the central nearside; an imaginary polyhedron drawn around this region covers only 4.7% of the lunar surface. As our detailed knowledge of the Moon increases, based on studies of the lunar meteorites in combination with the samples of the previous collections, the scientific goals for the next generation of lunar missions will become clearer and the choice of new landing sites will be based on a coherent set of multidisciplinary results rather than the almost accidental choices of some of the pioneering Apollo flights.

EXPOSURE AGES AND COLLISIONAL HISTORY OF L-CHONDRITE PARENT BODIES.
Thomas Graf and Kurt Marti, Dept. of Chemistry, B-017, Univ. of Calif., San Diego, La Jolla, CA 92093.

The composition, fossil remnants of particle radiations and cosmic-ray reaction products tell us that meteorites in our museums once existed in the interiors or on the surface of bodies hundreds of kilometers in diameter somewhere in the solar system. Some of these bodies may have been turned to rubble by collisions long ago, but others may still survive today. The continuing supply of meteorites and of cosmic dust particles which intercept the orbit of the earth indicate that collisions are still taking place and small objects are blasted out of craters on parent bodies of substantial size, because the cosmic-ray records of meteorites tell us that they were shielded from cosmic radiation inside larger bodies for most of the time since they formed in the solar system 4.56 billion years ago. The cosmic ray record begins to accumulate in the meteoroids once they are ejected from the parent body and are exposed to the cosmic ray environment in interplanetary space until they are captured by the Earth, and after passage through the atmosphere the surviving fraction is recovered as meteorites.

Cosmic-ray exposure ages (T) measure the time meteoroids spend in space as small bodies. This time T is an important measure in pinpointing the location of meteorite parent bodies, especially if clustering of T values occurs, reflecting catastrophic events and the simultaneous injection of impact debris into similar orbits. Exposure ages of meteorites are calculated from measured quantities in sub-gram sized chips of individual meteorites, by dividing the (integral) amount of cosmic-ray produced reaction products of a suitable nuclide X by the production rate of nuclide X, which in turn may be obtained from cosmic-ray induced radioactivity measurements. Since primordial noble gases in meteorites are very strongly depleted relative to non-volatile elements, stable nuclides ^{3}He, ^{21}Ne, and ^{38}Ar are particularly well suited to fill in for nuclide X and in the following we will use T(^{3}He), T(^{21}Ne), and T(^{38}Ar) to represent exposure times as measured from the He, Ne, and Ar concentrations, respectively, their well established isotopic signatures and their inferred production rates.

Orbits of only a few meteorites are well known, but they all lie in the inner solar system, with aphelia in the region of the asteroid belt. Objects in such orbits will intercept the Earth's orbit as required, but have calculated half-lives of only tens of million years (1). Therefore, objects placed in such orbits in the early history of the solar system would have been swept up long ago, unless they were constantly replenished by a reservoir. Observed values of T for chondritic meteorites are about equal to calculated orbital lifetimes and show occasional clusters in their age distribution. Observed shock effects and some measured substantial losses of radiogenic ^{4}He and ^{40}Ar, gaseous products from the decay of ^{40}K, ^{232}Th, and ^{238}U, respectively, in the meteorites bear important

signatures for collisional events. All these clues point strongly to the asteroid belt as the reservoir producing most meteorites.

Fig. 1 is a histogram of the exposure ages of L-chondrites, a major class of ordinary chondrites. The distribution is shown on a logarithmic scale. We use a compilation of all He, Ne, and Ar measurements in meteorites (2). Not all the experimental data in this compilation are equally well suited to calculate exposure ages. Therefore we classify the data into three classes A, B, and C. The highest quality class A ages are believed to have an uncertainty comparable to the resolution of the histogram. We make the following observations:

- A peak at ~40 million years (My) is clearly resolved and only few meteorites have longer exposure ages than the ones belonging to this peak. Exposure ages around 40 My are quite high but still consistent with calculated collisional lifetimes for bodies in Earth-crossing orbits. Therefore a major catastrophic event is indicated by this peak. It is interesting to note that a peak at ~35 My and a clear drop-off was also observed in the exposure age distribution of the H-chondrites (3). However, according to our production rates, the two events appear to be distinct.

- A large fraction of L-chondrites shows significant shock effects and losses of radiogenic ^{4}He and ^{40}Ar. It was shown that several of these meteorites experienced catastrophic degassing ≤300 or ~500 million years ago, long before they were exposed to the cosmic-ray environment (4). Fig. 2 shows the age distribution of those L-chondrites which show large and similar losses of the radiogenic gases ^{4}He and ^{40}Ar ("degassed" L's) as well as the complement distribution (all minus "degassed"). We observe that "degassed" L's tend to have shorter exposure ages and that the 40 My peak is weak.

- A subgroup of the "degassed" L's that we call "late degassed" is characterized by even larger losses of radiogenic ^{4}He. The exposure ages of this subgroup, also plotted in Fig. 2, are < 13 My and peak at ~5 My. We notice that the ratios T(^{3}He)/T(^{21}Ne) are lower on average than either for L's or "degassed" L's. This indicates that some of the cosmic-ray produced ^{3}He was lost, and therefore also radiogenic gases ^{4}He and ^{40}Ar may have been lost during cosmic-ray exposure. Gas losses during cosmic-ray exposure can be caused by solar heating or by secondary collisions. Alternatively, the very low ^{4}He concentrations in some "late degassed" L's may be due to recent catastrophic events, as illustrated by the Malakal meteorite (a member of this subgroup) where the Ar data indicate that gas loss occurred ~50 My ago (4). Note, that within error limits this age is consistent with the 40 My exposure age peak.

- The complement distribution (all minus "degassed" L's) appears to be constant between 5 and 25 My and then drops off sharply. Furthermore, an age cluster of "degassed" L's is recognized at ~25 My. Therefore a distinct peak may account for this fine structure.

What do we learn from these observations? Some conclusions are briefly discussed:

1) Thousands of asteroids are known and could in principle contribute to the meteorite influx on Earth. On the other hand, only few parent bodies are required to explain the discontinuous properties of chondrites. The observed 40 and 35 My exposure age peak at the upper end of the age distribution of L- and H-chondrites indicates that our collection of meteorites may be strongly biased by a few large events.

2) Catastrophic losses of radiogenic gases occurred before the meteoroids were exposed to the cosmic-ray environment. Assuming a single asteroid for all L-chondrites, the observed differences in the exposure age distribution of L's, "degassed" L's and "late degassed" L's indicates either population discriminations in replenishing Earth-crossing orbits or differential orbital lifetimes.

3) Multi-stage histories of meteoroids can in principle explain such discriminations: During large collisional events major fragments and rubble are likely to be ejected from the parent body. Some of them may end up in Earth-crossing orbits and may subsequently be captured by the Earth without further fragmentation. Others undergo collisions and material which previously was shielded is exposed to cosmic-rays.

4) Secondary break-ups can sometimes be detected because the production rates of cosmic-ray produced nuclides depend on the shielding depth: shielding sensors such as the $^{22}Ne/^{21}Ne$ ratio may still remember the irradiation conditions of the meteoroid during the second last stage of irradiation, whereas measured radioactivities were mainly produced in the last stage. In the exposure age distribution of H-chondrites (3,5) we found a subgroup of H's which most likely have experienced complex irradiation histories: The $^{22}Ne/^{21}Ne$ ratios are lower than average indicating large shielding and this group's apparent exposure ages are <4 My. However, in the case of a two step irradiation (the first stage in larger objects) the calculated apparent exposure ages are in error, because the assumed production rates do not apply since they are too high. Bur Gheluai, one of these meteorites was recently studied in detail and at this conference there is a report which establishes a complex irradiation history (6).

5) Although ordinary chondrites are the most common type of meteorites captured by Earth (~85%), spectroscopists do not find good spectral matches for chondrites among the asteroids. A large fraction of the asteroids on the inner edge are of type "S" and resemble stony meteorites although no good matches are known (7). On the other hand the Apollo asteroid Toro appears to match the L-chondrite spectrum reasonably well (8). We should not rule out the possibility that the predominance of chondrites today is related to collisional destruction of parent objects. It seems possible that chondrite parent bodies were reduced by collisions to small objects.

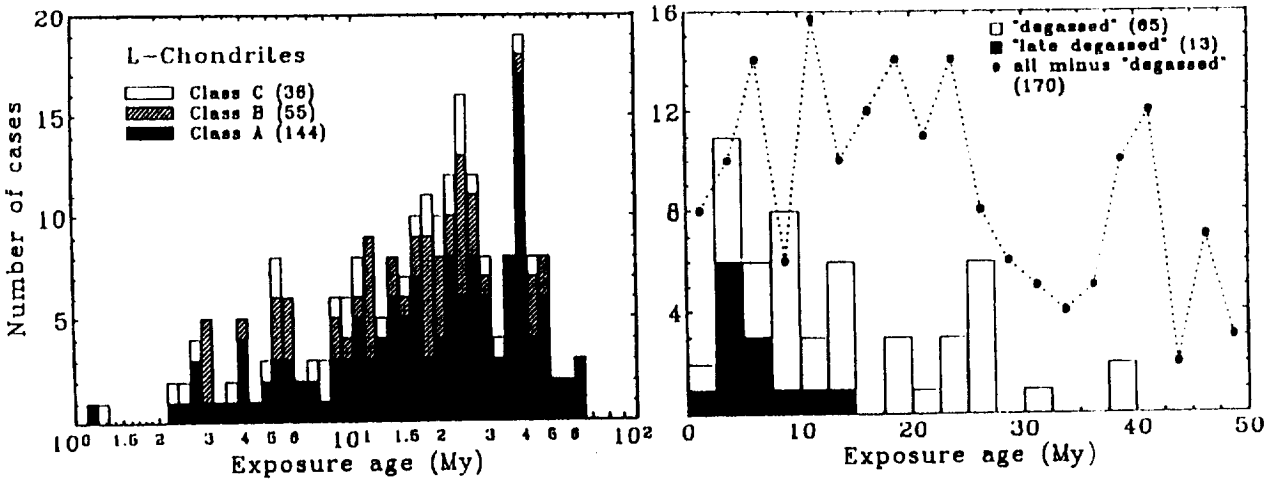

Fig. 1: Exposure age distribution of L-chondrites on a logarithmic scale, using an age resolution of 10%. Class A, B, and C represent quality classes (see text). The number of cases for each group is given in parenthesis in both figures.

Fig.2: Exposure age distributions of 3 subgroups of L-chondrites: (1) "degassed" L's with large and similar losses of radiogenic ^{4}He and ^{40}Ar; (2) "late degassed" L's (subgroup of "degassed" L's) with even larger losses of radiogenic ^{4}He; and (3) complement group (all minus "degassed" L's).

References:

(1) Wetherill G. W. (1974) Ann. Rev. of Earth Plan. Sci. 2, 303-331.
(2) Schultz L. and Kruse H. (1989) Meteoritics 24, 155-172.
(3) Graf Th. and Marti K. (1989) Meteoritics 24, 271-272.
(4) Bogard D. D., Husain L., and Wright R. J. (1976) J. Geophys. Res. 81, 5664-5678.
(5) Graf Th. and Marti K. (1989) Lunar Planet. Sci. XX, 353-354.
(6) Wieler R. et al. (1990) Lunar Planet. Sci. XXI.
(7) Bell J. D., Davis D., Hartmann W., and Gaffey M. (1989) in Asteroids II (eds. R. Binzel, T. Gehrels, M. Matthews) pp 921-945. University of Arizona Press.
(8) Chapman C. R., McCord T. and Pieters C. (1973) Astron. J. 78, 502.

LONG-SOUGHT PRIMORDIAL FINE-GRAINED INCLUSION DISCOVERED:

Beth B. Holmberg and Akihiko Hashimoto, Harvard-Smithsonian Center for Astrophysics, Cambridge, MA 02138, U.S.A.

Fine-grained inclusions, one of the many types of mineral masses which make up carbonaceous chondrite meteorites, have for some time been looked to as an important source of clues in understanding the earliest beginnings of the solar system. To date, the fine-grained inclusions studied have all been severely altered mineralogically and texturally. During recent studies of a sample of the Kainsaz meteorite, we have found a fine-grained inclusion which is apparently primordial-- unaltered in mineralogy and texture since its formation in the early solar nebula some four-and-a-half billion years ago.

Carbonaceous chondrites are one group of the stoney meteorites. They represent only about 1% of the total number of meteorites which have been found, yet for the last two decades they have provided much of the most valuable information used in deciphering the origin of the solar system. Some of the exciting finds in this class of meteorite have included the presence of amino acids distinctly different from those on earth, and micron-sized diamonds of interstellar origin!

Carbonaceous chondrites are dark gray to black meteorites with a variety of small (up to several millimeters) mineral masses visible throughout them. About 90% of the volume of the meteorite, including many of these masses and the bulk of the binding matrix, is composed mainly of magnesium- and iron-rich silicate minerals. The remaining mineral masses fall into two groups: some are coarse-grained, compact and well-rounded, the others are very fine-grained, porous, and more irregular in shape. Both are composed of minerals consisting mainly of calcium, aluminum, magnesium, silicon, and oxygen. These are referred to as coarse-grained and fine-grained calcium-, aluminum-rich inclusions (CAI's), or sometimes 'white inclusions'. The presence of calcium- and aluminum-oxides in minerals tends to raise their melting and boiling points significantly-- these are high temperature minerals.

Calcium-, aluminum-rich inclusions are important for study because they are generally considered to be some of the most primitive material in the solar system, having formed, even before the planets, directly in the solar nebula about 4.6 billion years ago. The early nebula consisted of a huge disk-shaped cloud of hot gases and minute solid dust particles. These gases, on cooling, began to condense to form mineral grains. This is a bit like breathing on a window in winter-- water vapor (gas) from your breath condenses and freezes on the surface of the window, forming ice (solid water). CAI's are believed to be the *very first* generation of solid material that existed in the nebula-- because of their high-temperature nature, they could survive the terribly hot environment of the nebula, and they could be some of the first minerals to condense from the nebular gases. Fine-grained inclusions are probably aggregations of these tiny, early condensate grains. As such, the chemistry, mineralogy, texture, and isotopic compositions of calcium-, aluminum-rich inclusions provide one of the best sources of information for deducing and understanding the chemical and physical conditions in the early solar nebula. Indeed, many of these inclusions even display isotopic signatures which may well represent nucleosynthesis events which occurred even *before* the formation of the solar nebula!

Despite this, fine-grained inclusions have seen somewhat limited study, probably due in large part to the difficulties involved with examining and analyzing them. Even with modern electron microprobes, it takes considerable effort and time to get decent images and analyses of the 5-50 μm grains which make up fine-grained inclusions. The micron-thick mineral layers which cover them are even more difficult to study. Those fine-grained inclusions which have been studied have had the common trait of being severely altered mineralogically. It is easy to understand this sort of thing happening in the changing chemical and thermal environment of the

evolving nebula. The theories involving their origins have relied on chemical similarities to coarse-grained CAI's to deduce the original mineralogy of fine-grained inclusions. Until now, however, no unaltered, unmetamorphosed fine-grained inclusion had been found for study.

In a thin section (~1.5 cm x~1.0 cm; 30 μm thick) of the Kainsaz meteorite we recently found a white, elongated (2.2 x 0.8 mm), fine-grained inclusion. Kainsaz, found in the U.S.S.R., is one of the least metamorphosed meteorites of it's class (CO3). The inclusion, named K-1, is an irregular mass of loosely-packed spinel grains, generally 5-30 μm in size. Each of the spinel grains is coated with a layer of melilite, occasional anorthite, and very thin pyroxene, totalling only a few microns of thickness (fig. 1). The spinel ($MgAl_2O_4$) contains 1-5 wt% FeO (replacing MgO in the mineral structure), though grains with up to 15 wt% FeO may be found towards the outside of the inclusion. Spinel occupies about 45% of the volume of the inclusion. The combination of spinel-covering minerals (melilite+anorthite+pyroxene) accounts for about 25% of the volume of the inclusion. The remaining 30% is void space (fig.2). This is the most spinel-rich and porous fine-grained inclusion that has been found. The entire inclusion is enclosed by an extremely fine-grained (grain size≤1 μm) two-layered rim composed mainly of iron-rich olivine (fig.3). This rim is about 80 μm in total thickness, and occasionally intrudes the inclusion, filling the spaces between spinel grains up to a depth of about 50 μm from the inclusion surface. Similar rim features are not uncommon on other fine-grained inclusions. They have been referred to as 'accretionary rims' and are apparently a secondary feature, forming independent of the accretion of the inclusion itself. This feature conjures a picture of the inclusion floating in the gases of the now-cooler nebula, collecting tiny particles of later mineral condensates on its surface, much like a cotton ball rolling across a dusty floor.

Previously studied fine-grained inclusions, primarily from the Allende meteorite, contain a much broader range of minerals. Many of these are considered to be secondary minerals produced by chemical alteration of the original Ca, Al-rich minerals. These secondary minerals are generally low-temperature in nature and carry volatile elements as additional constituents. This has cast some doubts on the idea of fine-grained inclusions as high-temperature nebular condensates. Yet certain isotopic signatures point to formation very early in the evolution of the solar nebula. If Allende fine-grained inclusions *are* alterations of some early high-temperature condensate, the original (pre-alteration) minerals are theorized to include melilite, anorthite, spinel, pyroxene, and perovskite. Remnants of most of these primary minerals have escaped complete alteration and may be found in the Allende inclusions. Melilite, however, is missing in all but one of the fine-grained inclusions thus far studied. In coarse-grained inclusions, melilite is the most abundant phase, and is seen, in places, to partially alter forming a mineral composition very similar to that of the fine-grained inclusions. No other coarse-grained CAI minerals are seen to alter to any great degree, indicating that melilite is the primary mineral most susceptible to alteration. The compact coarse-grained inclusions minimize the interactions with mineral-altering nebular gases, but the small grain size and abundant open space in fine-grained inclusions would allow extremely easy access of such gases to the primary minerals. If melilite is the most easily altered of these minerals, it makes sense that it might not remain in existence in most of the altered fine-grained inclusions. Other features of previously studied fine-grained inclusions include a distinctive three-fold zonation of bulk mineralogy, sort of like an onion, with each concentric layer having its own collection of minerals. This is a gross alteration feature controlled by the diffusion and chemical potentials of vapor species released from the existing calcium-, aluminum-rich minerals, and gas species still present in the nebula.

In spite of its abundant pore space, which would allow easy movement of mineral-altering gases into and through the inclusion, the K-1 inclusion shows signs of *not* having been subjected to the alteration experienced by other fine-grained inclusions. It utterly lacks the three-fold zonation of mineral composition seen in other inclusions. It does not contain any of the secondary minerals, produced by alteration, which are seen in other inclusions. Most importantly, it is rich in melilite, the mineral shown to be most susceptible to alteration. K-1's

overall chemical composition is still similar to that of other fine-grained inclusions, and, in fact, its mineralogy includes many of the anticipated original minerals. While the increased iron contents of some of the outermost spinel grains may be attributed to minor alteration effects, it would appear that K-1 has basically survived as a pre-alteration, or primordial, fine-grained inclusion.

How has K-1 managed to avoid the alterations seen in other fine-grained inclusions, and survive intact for so many eons? The first part of the answer is that various meteorites, even those of similar bulk composition, probably evolved in different parts of the nebula, and may, therefore, have experienced slightly different conditions. Secondly, parent body of the Kainsaz meteorite has avoided any significant thermal and mechanical processes since its accretion and has, therefore, apparently done a very effective job of sealing the inclusion off from outside influences and cradling its relatively fragile structure intact through the years.

One obvious question that comes is: does the K-1 inclusion represent a direct (unaltered) precursor of the altered fine-grained inclusions observed in Allende and other carbonaceous chondrites? Spinel-cored grains are fairly common in the Allende fine-grained inclusions. They tend to be covered by one to three mineral layers which may include nepheline, anorthite, grossular garnet, olivine, diopsidic pyroxene, and/or hedenbergite. The pyroxene layer is generally outermost on such grains. If K-1 were to be altered, the melilite layer would change to nepheline, sodalite, anorthite, and/or grossular. The anorthite found in K-1 would likely alter to nepheline and/or sodalite, and the spinel core to a mixture of olivine and nepheline. The outer layer of diopsidic pyroxene would tend to be unaffected. This looks to be in fairly good agreement with the alteration minerals found in Allende inclusions, but the hedenbergite found in Allende is unaccounted for. Hedenbergite, however, is considered to be a mineral formed by direct condensation from a gas onto a pre-existing mineral surface. It is, therefore, a secondary mineral, but not an alteration mineral.

Is there any reason to think, then, that K-1 is *not* an ancestor of the Allende fine-grained inclusions? Yes, there is. Allende inclusions have an abundance of materials filling the voids between spinel-cored objects. These materials consist mostly of tiny particles of the previously described alteration minerals, as well as diopsidic pyroxene and spinel. The volume of such in-filling material often is greater than the volume of the spinel-centered grains themselves. K-1 has much void space between spinel grains, but little material filling such space. To produce the textures seen in the Allende inclusions, K-1 spinel grains would not only have to be altered, they would also have to disintegrate to produce such volumes of space-filling materials. However, most of the spinel-centered objects in the Allende fine-grained inclusions appear to have maintained their textural integrity: the outermost pyroxene layer remains whole and fully attached to the rest of the grain.

Does this lack of complete correlation invalidate the usefulness of the K-1 fine-grained inclusion? By no means! While it is apparently not a specific precursor of the Allende fine-grained inclusions, it is still the most unchanged, primitive example of a fine-grained inclusion yet to be found. It is likely that further study on the variety of fine-grained inclusions in existence will turn up a descendant of the K-1 inclusion. Further, the finding of such a primordial inclusion in the Kainsaz meteorite points towards this and other less-metamorphosed carbonaceous chondrites as a likely place to search for an Allende inclusion precursor. Work on the K-1 inclusion is just beginning: further studies (including those of isotopic composition and rare-earth element enrichment) on this and any similar inclusions will help to further define the conditions and processes present in the early solar nebula.

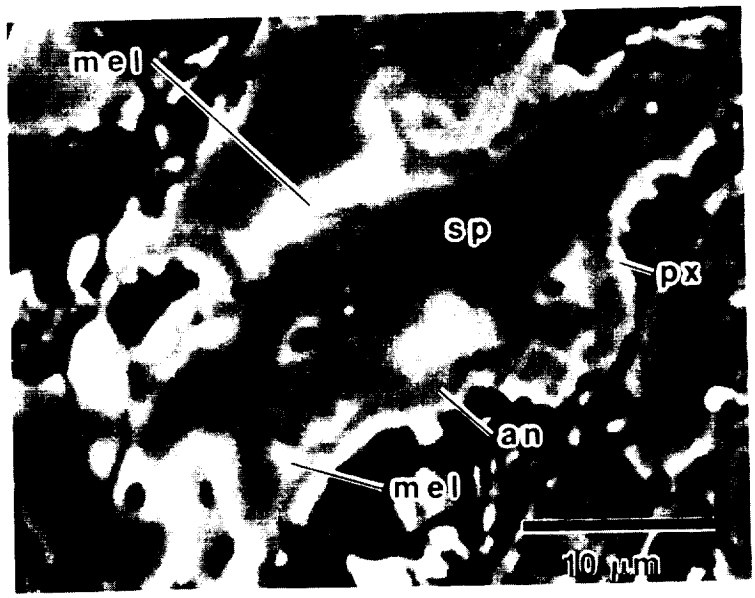

Fig. 1. One of the larger, more complex grains in the K-1 inclusion. The central spinel grains (sp) are coated by a layer of melilite (mel) of variable thickness, discontinuous anorthite feldspar (an), and a thin outer layer of pyroxene (px).

Fig. 2. The typical texture of the K-1 inclusion, showing irregular spinel grains loosely packed together. A thin layer of covering materials (melilite+anorthite+pyroxene) can be seen on each of the grains.

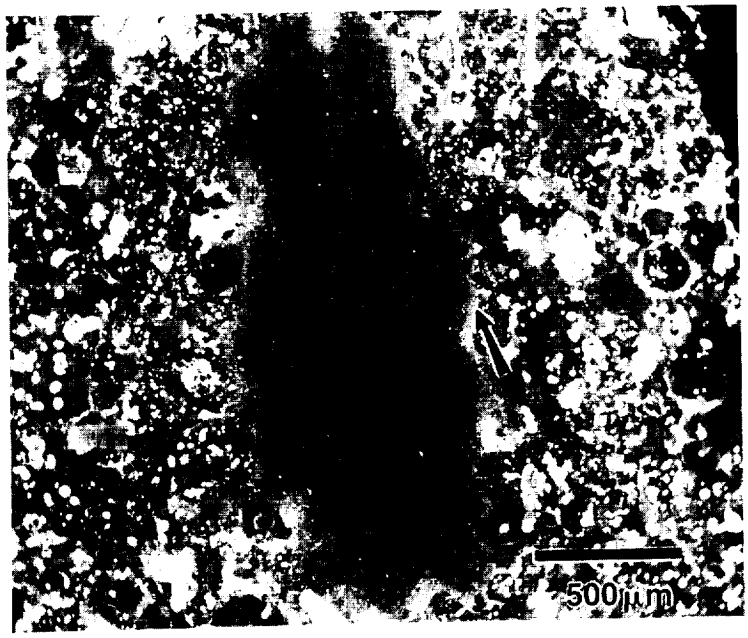

Fig. 3. The K-1 fine-grained inclusion. Note the irregular shape, consistant texture, and surrounding accretionary rim (arrow).

MODELS OF SOLAR-POWERED GEYSERS ON TRITON: R. L. Kirk,

U.S. Geological Survey, Flagstaff, AZ 86001

Introduction A highlight of the Voyager 2 encounter with the Neptune system was the discovery by Laurence Soderblom of the U.S. Geological Survey of actively erupting geyser-like plumes on Triton. A series of images from different viewing angles obtained as the spacecraft flew past Triton clearly shows at least two plumes above the satellite's surface. The plumes, which appeared dark relative to the surface beneath them, included a vertical column that rose to an altitude of about 8 km (5 mi), and a subhorizontal dark cloud that extended westward for several hundred kilometers. Other images revealed long, east-west clouds recognized as bright features over Triton's night side that were similar in form to the clouds attached to the eruption columns. Localized bright clouds were seen silhouetted over the day-side horizon in yet other images. These clouds may all be manifestations of the same eruptive phenomenon. Both the plumes and the clouds were located within the area of the south polar cap, at latitudes ranging from 30° to 60°S. This localization, combined with the fact that the current latitude at which the sun passes overhead is 45°S, suggests the eruptions are powered (or at least in some way triggered) by sunlight. I have been modeling solar-powered Triton geysers, seeking to understand (1) the processes that might be involved in channeling solar energy to an erupting geyser, (2) the size and properties of the subsurface region from which the eruptive fluids might be derived, and ultimately (3) whether solar energy could account for the observed eruptions on Triton.

Properties of the Geysers The possibility of currently active eruptions had been raised by Soderblom and other members of the Voyager Imaging Team earlier in the encounter with Triton, in an attempt to explain the many northeast-trending dark streaks seen on Triton's south polar cap. These streaks were found in the same range of latitudes where the active plumes were later discovered. The streaks strongly resembled dust streaks created by wind action on Mars, yet Voyager 2 measured the pressure in Triton's nitrogen atmosphere to be scarcely one one-thousandth the pressure of the Martian atmosphere. Soderblom and others suggested that gas erupted at a higher local pressure could carry dark particles that would be deposited downwind as a streak. The eruptive activity was thought to be very recent—to have occurred less than a few Tritonian years ago (each such year equals 165 Earth years). Otherwise the streaks would have been buried by nitrogen frost that condenses out of the atmosphere during the winter. It seems likely that the plumes later found are indeed related to the surface streaks. If so, we can use the relative numbers observed—roughly 10 plumes and clouds compared with perhaps 100 streaks—to estimate the length of time when any given plume is active: about one-tenth of the Tritonian summer, or 5 to 10 Earth years. The difference in trend between the plumes and streaks does not rule out their being related. A model of Triton's atmosphere by Andrew Ingersoll of Caltech predicted that the wind direction changes from northeast to west with increasing altitude. The plumes observed in action apparently reach the uppermost, westward-blowing layer of the atmosphere. Streaks that extend northeast from dark spots (presumed to be sources of vent areas) may be formed by less energetic eruptions that reached only the northeast-blowing atmospheric layer.

It is possible to estimate the amount of material being erupted. Both the horizontal parts of the plumes and their shadows appear about 5% darker than the surrounding surface. This suggests the suspended dust is nearly black and is abundant enough to intercept 5% of the light passing through the plume. Combining this observation with an estimate of the size of the dust particles (they must be big enough to absorb light efficiently, but not so big that they settle out of the plume), the radius of the plume, and the wind velocity from Ingersoll's model, Soderblom has calculated that about 1 kg (2 lb) of dust must be erupted per second. The amount of gas erupted is harder to estimate directly, but it might be roughly 20 times the amount of dust.

Susan Kieffer of the U.S. Geological Survey applied a fluid-dynamic model, developed to describe the eruption of terrestrial geysers and volcanoes, to the plumes on Triton. She found that the height of the Tritonian plumes could be accounted for if they were about 100 m (330 ft) across at the base, and if the erupted nitrogen gas were at a temperature of roughly 41 K (−386°F) before it expands and cools to the ambient temperature of 37 K (−393°F). Eugene Shoemaker, also of the U.S. Geological Survey, has pointed out that the geyser source to which the 100-m size applies is more likely on geological grounds to be a region of many closely spaced fissures or vents rather than a single large opening. If the height of the plumes is limited by a stratified layer in the atmosphere, a larger source diameter would be consistent with the observations.

TRITON GEYSER MODELS: R. L. Kirk

A Greenhouse on Triton A partial model of a solar-powered Tritonian geyser was described in the 30-day report of the Voyager Imaging Team [SMITH, B.A., *et al.* 1989, *Science*, 246, 1422–1429]. In this model, solar energy is absorbed by dark material underlying a transparent surface layer of nitrogen ice. The low thermal conductivity of the nitrogen leads to a strong "greenhouse effect": the temperature, and hence the equilibrium vapor pressure of nitrogen, are greater below the layer than at the surface. If the nitrogen layer forms a gas-tight seal (it was suggested), a reservoir of pressurized gas might be built up in pore spaces below the surface. Rupturing of the seal, or lateral migration of the gas to regions where the seal is imperfect, would lead to venting of the trapped gas that might account for the observed eruptions.

Preliminary calculations by Robert Brown, Jet Propulsion Laboratory, and others indicate that the greenhouse mechanism could generate the required temperature increase. The intensity of sunlight at Triton is only one one-thousandth of that at the Earth, or about 1.5 watts per square meter; averaged over one Triton day, the power incident on an area near the subsolar latitude is roughly half as great. If this power were deposited at the base of a 2-m thick nitrogen layer and all of it were conducted upward, the temperature at the base would be 7.5 K higher than that at the surface. The temperature enhancement would be less if (as is likely) some of the sunlight were reflected, or if a significant amount of heat were conducted away from the greenhouse downward or horizontally.

Even if the greenhouse were perfect, so that all of the solar energy incident on it could be used to vaporize nitrogen to feed the geyser, a region 1.5 km (about 1 mi) in radius would be required to collect enough energy. If the loss of energy by conduction through the greenhouse layer is allowed for, the required radius increases to 4 km, or almost 100 times the inferred radius of the geyser source regions. Thus, for the insolation-driven geyser to work, energy must be transmitted to the geyser source region from a much larger surrounding "collector." This energy must be transmitted by a means that is much more efficient than thermal conduction in solid nitrogen; otherwise, conduction across the greenhouse layer would "short circuit" the geyser.

Energy-Transport Processes My investigations have indicated that, although the thermal conductivity of water ice is roughly 100 times greater than that of solid nitrogen, conduction in a water-ice layer could not transport the energy required for a Tritonian geyser. A much more promising means of energy transport is the flow of gas through pore spaces in the material below the greenhouse layer. Consider a localized region of the subsurface that is warmer than its surroundings. The gas pressure and density in the pores in this region will be enhanced in keeping with the equilibrium vapor pressure of solid nitrogen as a function of temperature. The pressure difference between the warm region and its surroundings will drive a flow of gas through the interconnecting pore spaces; in order to maintain the equilibrium pressure distribution despite this flow, nitrogen will evaporate in the warm region and condense where it is colder. Energy, in the form of latent heat, will consequently be transferred from one region to the other. This energy transport is in the same direction as ordinary thermal conduction, and one can define an "effective thermal conductivity" that describes the energy flow for a given temperature gradient. Unlike the ordinary thermal conductivity, however, the effective conductivity increases dramatically with temperature because of the strong temperature dependence of the vapor pressure and density. The mechanism of heat transport just described is the same as that employed in "heat pipes," hollow tubes containing a wick and a volatile liquid in equilibrium with its vapor, which are variously used for such purposes as controlling the temperature of spacecraft and baking potatoes more efficiently.

In addition to intrinsic properties of the gas, such as vapor pressure, latent heat, and viscosity (which determines the rate of flow under a given pressure gradient), the effective thermal conductivity depends on the permeability of the porous medium. The permeability is a measure of the ease with which fluid can pass through the pores; it is a function of the fraction of the total volume the pores occupy and of their size. I used a theoretical model relating permeability to porosity and to the size of the solid grains or blocks (on which the size of the pores depends) to calculate the effective conductivity of a porous nitrogen layer on Triton. To obtain reasonable success with the thermal models described below, I found it necessary to assume quite large grain sizes. For example, the numerical results I give here are for a grain size of 2 m (about 6.6 ft) and a porosity of 10%. The corresponding effective conductivity at the subsurface temperature of 41 K is about 4000 times the conductivity of non-porous nitrogen at the same temperature and roughly twice that of copper at room temperature.

The permeability required to achieve this effective conductivity is very large compared with reported

permeabilities of terrestrial rocks and sediments, but this may be a matter of observational bias. Deposits of meter-sized boulders exist on Earth, but such deposits are so permeable that they are of little hydrologic importance, and their permeability is unlikely to have been measured; there is no real reason to suspect it is not as large as theory predicts. There is, moreover, a mechanism that might maintain a very porous and coarse layer of nitrogen on Triton's surface. The global equilibrium temperature of 37 K is only slightly above the temperature of 35.6 K (−395.6°F) at which solid nitrogen undergoes a phase transition. The lower-temperature phase is about 10% denser than the higher-temperature phase. Thus, if the temperature dropped only a few degrees below the equilibrium value during the winter, the solid nitrogen would contract and fracture, yielding roughly the 10% porosity assumed here. The fracture spacing (or block size) might well be comparable with the thickness of the nitrogen layer, making meter-sized blocks plausible for a layer several meters thick. Jostling of the blocks as they separated would ensure that the fractures would not reclose entirely when the temperature increased and the nitrogen converted back to the less dense phase.

Steady-State Thermal Models To understand the required geometry and size of a solar-powered geyser, I have calculated numerical models of the temperature field beneath the collector and geyser. I started with steady-state models, for several reasons. Steady-state models are simpler and faster to calculate than time-dependent ones, particularly for the temperature-dependent effective conductivity we are interested in. It is also possible to "scale up" the results of a single steady-state calculation to determine the temperatures in systems of different sizes; this is much less convenient for time-dependent models. Finally, steady-state models are realistic representations of two possible situations on Triton: a "reservoir" of gas and energy that has been created by the Sun but has not yet been tapped by a geyser, and a subsurface conduit that is receiving energy and passing it on to a geyser at an equilibrium rate. The geometry of my models is idealized: the collector is represented by a circular patch on the surface that supplies energy, and the geyser (if any) by a smaller concentric circle in which energy is extracted.

I also make an approximation of the method by which the greenhouse collector feeds energy into the subsurface region. In reality, a fixed amount of solar energy is absorbed at the base of the greenhouse, and the temperature adjusts itself so that thermal conduction upward to the surface and gas-phase transport downward together remove just this much energy, maintaining equilibrium. It is easier, however, to model two limiting cases of this behavior: (1) for a small collector, most of the energy is transported away by the gas rather than through the greenhouse, making it appropriate to specify the energy input into the subsurface; and (2) for a large collector, most of the energy is lost by conduction to the surface, making it appropriate to specify the temperature at the base of the greenhouse layer. Thus, in reality, the reservoir temperature achieved increases with size for small collectors, then levels out at a value controlled by the efficiency of the greenhouse layer. By comparing the two types of simplified models, I can estimate the size of the smallest collector that can approach the limiting temperature of the reservoir.

I assuming the effective conductivity described above and an energy input into the subsurface of $0.1\,W\,m^{-2}$. The remainder of the solar energy is reflected away and conducted across the greenhouse layer to maintain the elevated subsurface temperature. I then calculate that a collector 30 km (18 mi) in radius would be needed to reach a limiting temperature of 41 K. I have further assumed in this this calculation that the porous layer is very deep. It is more likely that the layer of high effective conductivity is relatively thin; in any event, the Tritonian summer is not long enough for thermal steady state to be reached in a layer thicker than a few hundred meters (1000 ft). Smaller collectors can reach the limiting temperature if the porous layer is thin. For example, if the layer is 100 m (330 ft) thick, a collector 3 km (2 mi) in radius suffices. This size is comparable with that of the dark spots seen at the bases of the active geysers on Triton.

An interesting feature of these reservoir models is that, although energy is transported primarily by gas flow, it is stored mainly as sensible heat in the solid matrix. The amount of pressurized gas actually present in the pore spaces when the reservoir is tapped is much less than the amount that can be released by evaporation and cooling of the warm solid nitrogen.

The steady-state power that can be delivered to a geyser in the center of the collector region is a function of the effective conductivity, the geyser radius, the maximum subsurface temperature, and the thickness of the porous layer. As we have seen, the maximum temperature reaches a limiting value for large collectors that we will assume to be 41 K. It is convenient that the effect of the porous layer thickness largely cancels out: in a thinner layer, energy is fed to the geyser through a smaller area, but the thermal gradients are correspondingly larger. For a given permeability, the power delivered to the geyser increases linearly with

the geyser radius. Requiring that this power suffice to evaporate 20 kg of nitrogen (the estimated amount of gas erupting from the active geysers) per second, I find that a geyser radius of 400–600 m (1400–2000 ft) is needed, depending on the exact numerical model I choose. These values are 10 times less than the required radius of a "leaky greenhouse" with no lateral energy transport below the surface, but they are still 10 times greater than the estimated source radius of the active plumes. The calculated radius is decreased if the effective conductivity is larger, but, as discussed above, I have already assumed a very large permeability for the subsurface layer. According to the permeability-grain size relation I have used, a grain size of 6 m is needed to reduce the required geyser radius to 50 m.

Discussion The following conclusions can be drawn from the work I have outlined. First, for the Tritonian geysers to be solar powered, they must have a very efficient means of transporting energy from a large collector region to a much smaller geyser source area. Second, such an energy-transport mechanism may exist in the form of gas flow through a porous subsurface layer; the permeability I have assumed for this layer is admittedly very large, but it might be maintained by fracturing due to seasonal phase changes in the solid nitrogen. Third, thermal modeling indicates that, despite the efficiency of the gas in transporting heat away, a reservoir at the required temperature can be established under a collector of modest size (a few kilometers in radius) provided the permeable layer is relatively thin. Finally, the thermal models also suggest that the gas-phase energy transport is probably not efficient enough to deliver the power required for a geyser to a small enough source region in steady state. Clearly, the next step is to examine time-dependent models, in which a geyser taps a pre-existing reservoir. The initial output of energy and gas will exceed the steady-state value, allowing the requirements for geyser radius, permeability, or both to be relaxed. It is also of interest to see whether time-dependent models can predict the estimated active life span of the eruptions (5–10 Earth years). A preliminary scaling calculation is encouraging in this respect: 5 years is about the time required for gas flow to extract the excess energy from a region about 100 m across. The length of time for which a geyser erupts most actively may thus be determined by the time required to extract the thermal energy (in excess of that of the steady state eventually achieved) in the area immediately surrounding the vent.

INSPECTION OF THE LONG DURATION EXPOSURE FACILITY AND PLANS TO CHARACTERIZE THE DUST ENVIRONMENT IN LOW-EARTH ORBIT

LDEF Meteoroid and Debris Special Investigation Group*.

INTRODUCTION The Long Duration Exposure Facility (LDEF) was deposited at an altitude of 250 nautical miles (nm) in April of 1984, for an intended exposure of 9 months. LDEF has now been retrieved at an altitude of 175 nm, after a total exposure time of 5.7 years. While this unexpectedly long exposure has compromised a few experiments, it has greatly enhanced the scientific return from most. LDEF provides an unparalleled opportunity for characterization of the effects of exposure to the low-Earth environment.

LDEF is a totally passive, cylindrical satellite 30 feet long and 14 feet in diameter. Experiments are accommodated in 84 modular trays, for a total exposure area of 130 m^2. For comparison, Solar Maximum Satellite blankets totaled 3 m^2 and were exposed for 4 years. LDEF was exposed in a gravity-stabilized orientation, with deliberate Earth-, space-, leading-, trailing- and side-facing directions. The 57 different experiments concern basic science (dust, debris, comic rays, interstellar gas, exobiology), spacecraft materials and thermal systems, power and propulsion, and electronics and optics. One quarter of LDEF surfaces are dedicated to dust and orbital debris experiments. However, to make maximum use of LDEF the Meteoroid and Debris Special Investigation Group (M&D SIG) has been organized to permit coordinated analyses of the additional surfaces not already part of dedicated meteoroid or debris instruments. This group is also responsible for the integration of all LDEF meteoroid and debris data (from both the Principal Investigators (PIs) and M&D SIG) into a single data base.

The first purpose of the M&D SIG is elucidation of the meteoroid and debris environment in low-Earth orbit, through characterization of total flux, trajectories, chemistry, mineralogy, isotopic composition and sources. The second purpose is to assess effects of impactors on spacecraft materials through examination of crater formation, projectile penetration and secondary ejecta production, on the widely varied materials and experiment configurations on LDEF.

DOCUMENTATION OF THE IMPACT HISTORY OF ENTIRE LDEF SATELLITE

It is essential to document the entire impact record of LDEF before the component experiment trays are removed to PI laboratories, because many PI analyses will be destructive. Therefore, we will photo-document every large (>1 mm) impact feature on LDEF (trays and structure) using a binocular microscope, digitizing video images for later analysis. We expect to find a few hundred such features. We will also participate in the analysis of approximately 20 thermal protection blankets, which witnessed all pointing directions. Most of these blankets cover cosmic-ray detectors (sponsored by the Dublin Institute for Advanced Studies and the European Space Agency). We will also obtain components from several other experiment trays with desirable characteristics. The most

desirable materials that we have identified include low-density media, foils (stacked or otherwise), optical surfaces, very pure metals, identical materials facing in all directions, experiments with time-dependent mechanisms, and experiments with compartments or irregular geometries (for secondary ejecta and impactor penetration studies). This documentation will permit the population characteristics of the largest fraction of meteoroid and debris grains to be determined. We will present results of these initial inspections at the meeting.

DETAILED SCANNING AND ANALYSIS OF IMPACT FEATURES AND IMPACTORS

Selected surfaces will be completely scanned at high magnification on optical scanning tables located at the Johnson Space Center (JSC), the University of Kent and Langley Research Center. These data will permit the mid size-range impactor population to be evaluated. The smallest population of impactors will be characterized by electron optical techniques at the host laboratories of several M&D SIG members and LDEF PIs. Impactor residues will be characterized by a combination of electron beam, ion probe and microparticle INAA techniques (to mention a few).

In many instances, PIs not belonging to the M&D SIG will encounter impact features on their experiment trays of potentially great interest. Where it is impossible for the M&D SIG itself to analyze such features we will mitigate the potential data loss by providing the PI with advice and analytical standards, ensuring that all meteoroid and debris data collected by any LDEF worker will be internally consistent.

DATABASE AND CURATION Meteoroid and debris data collected by PIs will be combined with M&D SIG data into a single database. This database will be maintained by personnel of the Planetary Materials Curatorial Facility at JSC, guided by experience with the Solar Max Database. This database will be available for use by researchers and engineers, and will constitute a baseline for future spacecraft design efforts. Selected impact features of particular interest will be curated at the Curatorial Facility at JSC, along with a representative selection of materials flown on LDEF, serving as a valuable future source of information on the environmental effects of space exposure.

DATA INTERPRETATION The meteoroid and debris data will be used to make flux calculations and spacecraft hazard predictions. The directional nature of LDEF will permit particle trajectories to be included in these calculations, representing a significant advance over what was obtained from all previous investigations, including those of the Solar Max thermal blankets and louvers.

* W.H. Kinard (NASA/LaRC, Chair), M.E. Zolensky, F. Horz, D. Kessler, H. Zook (NASA/JSC), T.H. See (Lockheed), C.G. Simon, R. Walker, E. Zinner (Washington U.), D.R. Atkinson (Kirtland AFB), M.K. Allbrooks (S-Cubed), J.A.M. McDonnell (U. of Kent), D. Humes (NASA/LaRC), D. Brownlee (U. of Washington), J-C. Mandeville (CERT), M.M. Finckenor (NASA/MSFC), V. Chobotov (Aerospace Corp.), T. Bunch (NASA/ARC), M. Mirtich (NASA/LRC).

THE HEATING OF SMALL ROCKY BODIES IN THE EARLY HISTORY OF THE SOLAR SYSTEM: WHAT DO METEORITES TELL US? T.J. McCoy, G.J. Taylor, E.R.D. Scott and K. Keil, Institute of Meteoritics, University of New Mexico, Albuquerque, New Mexico 87131 USA.

Meteorites are naturally occurring objects that come from space and reach earth in pieces large enough to be recovered. Meteorites can be divided into two broad categories: those which have been melted and those which have not been. This melting occurred in asteroids (small bodies between Mars and Jupiter and source of most meteorites), not during passage through the earth's atmosphere. The meteorites that have not been melted were nevertheless heated. This heating is reflected in chemical and textural changes.

All unmelted meteorites are classified as chondrites, which contain chondrules (millimeter-sized silicate spheres). Ordinary chondrites, so-called becausee they are the most common group of chondrites, can be divided into 3 groups (H, L, and LL) which formed on three distinct bodies. The effects of this gentle heating in ordinary chondrites include homogenization of the compositions of the chondrule silicates, a general increase in grain size, and obliteration of chondrule boundaries. These changes are used to classify chondrite into a petrologic sequence, which ranks ordinary chondrites from type 3 (least affected by heating) to type 6 (most affected by heating).

Meteoriticists are particularly interested in determining the maximum temperature a meteorite reached and how quickly it cooled. This can provide information on the timing of heating relative to the formation of the asteroids and the sizes of the asteroids. One widely used method involves the exchange of nickel between two metallic minerals. As a meteorite cools, a low-nickel mineral (kamacite) grows and replaces a high-nickel mineral (taenite). The kamacite transfers its nickel into the taenite. However, nickel atoms migrate through kamacite much faster than through taenite and they tend to pile up as they enter the taenite. If a meteorite cools very quickly, the nickel atoms have less time to move into the middle of the taenite grains. Conversely, slow cooling allows nickel atoms to move into the center of taenite grains. As a result, a relationship exists between a taenite grain's size and the nickel content of its center. This relationship

allows measurement of how quickly a meteorite cooled - its metallographic cooling rate. Measurements of these cooling rates, as related to petrologic type, can tell us a great deal about how asteroids were heated.

One popular model for the heating of asteroids is the "onion-shell" model, where petrologic types would occur in shells around the center of asteroids, just as layers on the center of an onion. In this model, asteroids were internally heated by the decay of short-lived radioactive elements, and the maximum temperatures a meteorite reached decreased as distance from the center of the asteroid increased. Other authors believe that asteroids were heated from outside, possibly by a sun that was much hotter and brighter than it is now. If this were the case, we would expect the type 6 material to be located on the outside of the asteroid and cool the fastest. This situation is analogous to a rock in a campfire. The outside gets hottest in the fire, but when removed from the fire it cools the fastest. However, no correlation has been found between metallographic cooling rates and maximum temperature and neither model seems reasonable.

This lack of correlation has been used as evidence to develop an exotic, yet entirely plausible, model for the heating of meteorites. Most of the effects seen in ordinary chondrites occur near the maximum temperature, but metallographic cooling rates are established at lower temperatures for most of these meteorites. Consequently, some authors argue that the temperatures for these two events must have been reached when the meteorite was at different depths in the asteroids. This could have happened if the maximum temperature were reached in smaller asteroids, which then combine to make bigger asteroids. The metallographic cooling rates are then determined by the small asteroid's final resting place inside the big asteroid. Alternatively, the breakup and reassembly of an onion-shell body during metamorphism could cause a lack of correlation. In this case, the maximum temperature is dependent on depth, but before metallographic temperatures are reached, the asteroid is broken up and reassembled into a jumbled rubble pile. Once again, the metallographic cooling rates for a meteorite depend on where it was inside the reassembled asteroid.

HEATING OF ASTEROIDS

McCoy, T.J. *et al.*

In this work, we found for the first time a relationship between metallographic cooling rates and petrologic type in a small group of ordinary chondrites (the LL ordinary chondrites of petrologic type 3-4). This group of meteorites was chosen because the maximum temperature is in the same range as temperatures at which cooling rates were established. Thus, the maximum temperature and cooling rate must have occurred in the same environment. In this group, the hotter the meteorite got, the quicker it cooled. This is the trend expected for a body heated from outside. However, the slowest cooling rates (~1°C/Myr) require that the asteroid must have been big - much larger than could be heated by an external source.

An alternative explanation involves changes in the physical properties of meteorites brought about by the heating. Meteorites likely formed as a fluffy pile of their components and heating would cause the pile to compact and grains would grow together. As it compacts, the ability to cool increases. This might explain why the hotter material cooled faster. To prevent exchange of heat between different materials and ironing out of this trend, uneven heating may have been necessary. Localized pockets would be heated but be separated by much colder rock between the pockets. This implies that no systematic spatial relationship existed between petrologic types in at least some asteroids. Since this trend exists in only a limited range of petrologic types (3-4), it also implies that other petrologic types formed on other bodies. The small asteroids may have all accreted into a larger asteroid after cooling.

This work suggests that no systematic relationship exists between the location of a meteorite in an asteroid and the extent to which it was heated or cooled. Instead, heating of small bodies in the early solar system was a complex process which is not fully understood.

TRITON'S POST-CAPTURE THERMAL HISTORY *or* HOW LONG DID TRITON STAY MOLTEN, AND DOES THIS HAVE ANYTHING TO DO WITH HOW TRITON LOOKS TODAY? William B. McKinnon and Lance A.M. Benner, Department of Earth and Planetary Sciences and McDonnell Center for the Space Sciences, Washington University, Saint Louis, MO 63130.

Among the major highlights of last summer's Voyager encounter with Neptune were the first close observations of the mysterious moon Triton. Planetary scientists had long suspected that Triton would be interesting because of its anomalous retrograde (backwards) orbit, but Triton's surface turned out to be nothing less than astonishing: the satellite is covered with fractures, icy lava flows and volcanic calderas (collapse craters), frost and plume deposits, and other features that remain puzzling. Subsequent analysis revealed ongoing volcanic eruptions or geysering, with probably methane and/or nitrogen gas being vented. Thus Triton, the first icy satellite of its size class in the solar system to be visited by spacecraft, is a geologically active world, and one that possesses features that have, by and large, never been seen on the other icy satellites of the solar system.

What can explain this diversity of features? What does it mean for Triton's composition, structure, and history? And what does it all mean for how the outer solar system assembled 4.5 billion years ago? These are the questions planetary scientists will struggle with in the years to come. At this meeting, William McKinnon and Lance Benner of Washington University (in St. Louis) present the results of recent calculations and modeling that suggest that massive tidal heating and melting, associated with Triton's capture by Neptune, could be largely responsible for Triton's geologically youthful appearance.

Background

Several workers, going back many years, have suggested that Triton's retrograde and tilted (with respect to Neptune's equator) orbit could be explained if Triton was a captured satellite. There are two two major ways for this to happen. The first is capture by *gas drag*. This was first suggested by James Pollack and co-workers at NASA-Ames Research Center in 1979, and involves a solar-orbiting Triton passing close to Neptune when the planet was forming and thus when it had a large amount of gas (mainly hydrogen and helium) in close proximity. Gas drag would slow Triton down just enough that it would become permanently gravitationally bound to Neptune. A more modern and detailed version of the gas drag hypothesis is presented by Andrew Leith and William McKinnon in a companion talk in the Triton session. In that work, Triton is captured by gas drag in a later

phase of Neptune's evolution, one in which accretion of the planet is largely over, but in which there remains a compact disk (or nebula) of gas and solids that can form a satellite system similar to that which exists today around Uranus. The remnants of this original Neptune satellite system are seen close to Neptune. In any event, Triton passes through this disk, and is slowed enough to be permanently captured.

In all gas drag models there is substantial orbital evolution, due to gas drag, after the initial capture. In principle, Triton's orbit can shrink and completely circularize, attaining close to its present orbital configuration by gas drag alone. In fact, unless gas drag evolution halts, Triton's orbit will continue to decay, and it will eventually be torn apart by tides when it is very close to Neptune. This has not happened, of course, and thus gas drag models rely on the gas near Neptune being dispersed (such as by the T Tauri wind that is thought to have cleared away the solar nebula) before this could have happened, leaving Triton stranded in a retrograde, but uncircularized orbit. This is most plausible if Triton is captured close to the end of Neptune's accretion, so the version of the gas drag model by Leith and McKinnon is favored on this point.

Leith and McKinnon also show that gas drag capture by a protosatellite disk is favored because the time scale for gas drag evolution can be prolonged by two effects, thus making it more likely that Triton outlives the gas. The first effect is that solar perturbations cause Triton's eccentric and elongated capture orbit to markedly oscillate. Specifically, the point of closest approach, or pericenter, of Triton's orbit varies such that sometimes it is within Neptune's disk or nebula, and sometimes it is outside. If it is outside, then Triton's orbit doesn't evolve by gas drag at all during that orbit, and the overall effect is that Triton can take more than 10,000 years to spiral in. Furthermore, Triton is sufficiently massive compared with the estimated mass of the Neptune disk or nebula that it may be able to clear out zones or lanes within the nebula. Once this happens gas drag evolution will halt altogether. From this point on, Triton's orbital evolution will be controlled by tides (the topic of the talk by McKinnon and Benner), and be much slower.

The other capture mechanism is *collision* with an original "regular" Neptune satellite (one that would have formed from the Neptune nebula above). This was proposed by Peter Goldreich and co-workers at Caltech last year. Here, a collision, after Neptune's satellite system has formed, causes Triton to move from solar orbiting to Neptune orbiting in a single (cataclysmic) step. All further evolution is controlled by tides, or possibly by further collisions (and actually, during orbital evolution by gas drag, collisions may also occur with satellites that have formed or are in the process of forming). The post-collision orbit is a very elongated ellipse, taking Triton from several Neptune radii (R_N) from the planet to

possibly greater than 2000 R_N. The post-gas-drag orbit would likely be similar, but not so elongated.

Tidal Heating

McKinnon was the first to point out, in a 1984 paper in the British journal *Nature*, that a captured Triton would likely undergo massive heating as its orbit was circularized and shrunk by tides raised on it by Neptune. In that paper, Triton was estimated to have completely melted, with the most volatile components of its possible makeup (CH_4, N_2, etc.) being driven to the surface. These volatile ices had been identified spectroscopically at the time, and their presence on Triton's surface was confirmed by Voyager. The possibility of a Triton melted by tidal energy was reiterated by Goldreich and co-workers in their paper of last year.

The time scale of tidal evolution is an important quantity to estimate. The simplest model of the dissipation of tidal energy assumes that Triton remains solid throughout its orbital evolution. It predicts that a Triton with an extremely elongated elliptical orbit, extending to the edge of Neptune's gravitational sphere of influence, takes almost 10^9 yr to evolve inward and have its orbit circularize. This is significant because (1) the time scale is more than twice as long as predicted in McKinnon's 1984 paper (because Triton's radius was then unknown but thought to be near 1750 km, whereas it is now known to be a much smaller 1350 km) and (2) the time scale is much longer than the estimated duration of heavy cratering in the outer solar system (~500 million years). Therefore, the "new," smaller Triton could have stayed hot well beyond the era of heavy cratering, and it could be predicted that little if any of the heavily cratered terrains seen on nearly all of the other icy satellites would be observed on Triton by Voyager. (It is significant that the icy satellites without heavily cratered terrains are Europa, Enceladus, and Ariel, all of which are being or have been tidally heated.)

These simple models, which assume that Triton remains solid, cannot be correct in detail, because so much of Triton's orbital energy is dumped into the satellite that it must melt. More complex models are necessary, the subject of this LPSC talk.

McKinnon and Benner first determine how soon Triton begins to melt once tidal evolution starts, that is, after the capture collision or after gas drag evolution ceases. It turns out that Triton is so rock-rich, approximately 70% rock by mass with the other 30% being ices, that it is likely that Triton would begin to melt its ice and unmix, or differentiate, spontaneously, because of the energy liberated within the satellite by radioactive element (U, K, and Th) decay. Only by deliberately choosing parameters that lower Triton's internal viscosity is it possible to build an internal model of Triton that convects without melting.

TRITON'S THERMAL HISTORY: **McKinnon W.B. and Benner L.A.M.**

However, even for very elongated initial orbits that extend to the edge of Neptune's sphere of influence, the tidal energy dissipated during individual passes close to Neptune is, time-averaged, comparable to the power due to radioactive element decay. Therefore, it is very unlikely that melting can be significantly delayed. Only if Triton is captured cold will melting be put off, perhaps ~100 m.y. The best estimate is that Triton will begin to melt promptly. Incidently, Triton's rock abundance is very similar to that of slightly smaller Pluto, which is further evidence that Triton was born in solar orbit and was then captured.

Melting and differentiation are interesting because they are partially self-sustaining. The gravitational energy of unmixing liberated (by moving rock to the center and ice to the outside) is approximately 30% of that needed to melt Triton's ices. Therefore, continued radiogenic and tidal heating are necessary to push Triton all the way to complete differentiation. This is greatly aided by the fact that the tidal dissipation in a differentiating body increases wildly compared with that in a solid one. The dissipation increases because of abundant "hot" ice (ice near the melting point), transient multiphase regions such as ascending slush and descending mud diapirs, and because the opening up of an internal ocean allows greater tidal flexing. Calculations suggest that Triton will differentiate in under 10^7 yr, and possibly much less. The result is a liquid water ocean, approximately 350–400 km deep, capped by a thin, conductive ice shell, overlying a rock core.

Continued tidal heating in the core causes it to heat up and melt as well. The ultimate tidally heated configuration for Triton is nearly totally molten. A thin water-ice shell tops a liquid water mantle, and thin rock shell tops a liquid silicate core; this lower shell may be negatively buoyant, though, and may turn over as on a lava lake. There may be an inner core of liquid iron-sulfur, but no iron shell because the freezing point of the core is less than that of the molten rock mantle. We ignore for the time being any other ices, such as methane (CH_4) and nitrogen (N_2), that might form a surface ocean.

Once Triton melts, and it needs only a small portion of the total orbital energy potentially available to it, its orbital evolution actually slows. This seeming paradox results from the fact that dissipation in a liquid Triton is largely confined to the thin solid shells described above. The hot, near-melting portions of both shells are quite dissipative under tidal forcing, but the shells are at most only a few km thick. Of course, tidal flexing is at its maximum for a liquid body, but the total effect is still to stretch out Triton's orbital and thermal evolution due to tidal heating. Thus McKinnon and Benner conclude that a nearly totally molten Triton may stay hot for an extended length of time, greater than 500 million years. Therefore, as with the simple model of tidal heating above, it is predicted that Triton should not have retained any early record of heavy cratering. This conclusion was originally presented by McKinnon at the Fall 1988 AGU Meeting, in advance of the

Voyager Neptune encounter, but the results presented at this (LPSC) conference take advantage of the new knowledge of Triton's size and mass.

The Evidence from Triton

The question now is whether tidal heating and melting are *required* to explain the absence of heavily cratered terrains on Triton. This depends on the composition of the surface. If at least portions of Triton's surface are made of close to pure water ice, as in the models discussed here, then ancient craters could survive in these cold, rigid regions in the absence of tidal heating and associated geologic activity. Thus tidal heating would be required to explain Triton's present appearance. If, however, there is a crust of lower melting point ices (such as nitrogen and methane, mentioned above) greater than a few km thick, then continuing volcanic and other activity in this relatively soft layer driven by present-day radiogenic heating inside Triton could, by itself, probably destroy any ancient crater population. In this case, tidal heating is not required. Hence, in order to use Triton's appearance to determine whether massive tidal heating actually occurred, detailed geological analyses will be necessary to constrain the composition of Triton's surface layers.

Further work should also involve more detailed characterization of the volatile ices during the tidal heating epoch. This may lead to new constraints on the amount of tidal heating Triton experienced. During the time when Triton was mostly liquid, a surface ocean of CH_4 and N_2 liquid probably existed, overlying the water-ice shell described above. It may have been capped by a CH_4-ice shell, but this would have been too thin to affect the tidal heating and orbital evolution of the satellite. However, a tidally heated Triton would have a hotter surface than it does now, which means a substantial CH_4–N_2 greenhouse atmosphere, so it may have been too hot for surface methane ice.

There are many questions for the future. What chemical processing occurred in the hotter, thicker early atmosphere, and could this be linked to the absence of atmospheric carbon monoxide (CO) today? CO is predicted to occur, based on the composition of comets, and a captured Triton may represent the largest surviving cometary body known in the solar system. What chemical processing occurred in Triton's early water ocean? What happened to the abundant organic material that was likely a part of the satellite (>10% by mass according to the cometary model) during the era of extreme tidal heating? Study of this marvelous moon is only beginning.

A MODEL FOR CHEMICAL EVOLUTION OF LIFE ON MARS, V. R. Oberbeck, NASA Ames Research Center, Moffett Field CA, 94035, J. R. Marshall, Arizona State University, Tempe AZ, 85287, D. E. Schwartz, SETI Institute, Mountain View CA, 94043

For many years, man has been intrigued with the possibility that life might exist elsewhere in the universe and, in particular, on the planet Mars. Much of the interest was generated by the work of Percival Lowell who made elaborate maps showing a supposed network of canals on the planet's surface. Of course, recent space missions have shown no such evidence of canals constructed by advanced civilizations. They have, however, shown river-like channels on much of the planet's surface and a variety of different types of terrain. The river-like channels provide evidence that at some time in the planet's history water was present at the surface. This, combined with numerous other facts, persuaded many that Mars was the best planet to search for evidence of life. Consequently, the Viking missions were conceived and several experiments were conducted to look for evidence of life at the landing sites. Most of the data taken during these experiments have been interpreted to be inconsistent with biological activity[1]. For example, one of the Viking experiments attempted to test for the presence of life in soil samples by feeding nutrients to the supposed organisms in order to test for the production of carbon dioxide. The experiments were developed under the assumption that carbon-based life, like that on Earth, would produce carbon dioxide as a metabolic by-product. When the experiments were performed on Mars at the Viking lander sites, carbon dioxide was emitted from the soil samples, but the control samples (that were sterilized to kill any potential Martian organisms before the nutrients were added) also produced carbon dioxide. Because the Viking experiments gave no conclusive evidence that life existed at the surface of Mars, many took this to mean that life could never have originated on the planet.

Recently, new results in the scientific fields of astrophysics, planetary geology, and planetary meteorology and climatology have encouraged us to remain optimistic about the possibility that life might have originated on Mars in the distant past. It is now believed that liquid water was present in the very earliest geological periods of both Earth and Mars, and water is, of course, one of the major requirements for life as we know it. The theory for the origin of life, by chemical evolution, involves the production of complex organic compounds from initially simple ones like amino acids. These organic compounds could have been produced by processes occurring in the atmosphere in accordance with some recent scientific hypotheses. Alternatively, they could also have been brought into the early atmospheres of Earth and Mars by comets and interplanetary dust.

A current hypothesis suggests that large impacts of planetesimals or asteroids during the earliest period of history of both planets would have interrupted the process of chemical origination of life[2,3,4]. Giant impacts may have frustrated the establishment of life on Earth by sterilizing the entire planet; this probably occurred several times before life could establish its current ancestry. The time between such giant impacts just before the oldest evidence of life on Earth (3.8 billion years) has been used to estimate the maximum time required to originate life[3]. This time interval could have been as short as 2.5 million years just before 3.8 billion years ago. Thus, life on Earth may have been able to originate very rapidly in an

apparently hazardous impact environment. It has been proposed that the time available between planetary sterilizing impacts on Mars exceeded the time required to originate life on Earth. It is noteworthy that these favorable time windows occurred during the geologic period before surface water and prebiotic reactants vanished on Mars (3.8 billion years ago)[4]. Thus, even the existence of a heavy bombardment of planetesimals or asteroids on Mars would not necessarily have prevented the origination of life.

Mars remains the most likely extraterrestrial planet upon which life could have originated. For this reason, we are motivated to renew our search for life on Mars. Our experience from the Viking mission, however, teaches us that the search will be a very difficult one. If life does exist on the planet, it is difficult to detect using indirect sources of evidence. If life did exist at one time, and now is extinct, fossil evidence may be buried or scarce and difficult to locate. Any life existing on the planet today is probably beneath the surface and will be difficult to recover. This search can be made a good deal easier if we had some idea of the geological conditions that favored the origin of life because we would then know where on the planet to search for the evidence. Although a great deal has been discussed about potential Martian life itself, until now no specific models have been forwarded that consider the geological processes that could have led up to the appearance of life.

We begin our model by defining the conditions on the planets' surface when the harmful impacting planetesimals and asteroids were least traumatic and while liquid water still existed at the surface. This time is just before 3.8 billion years ago at the end of the geological period referred to as the Noachian. During the first 800 My of the history of the solar system, all of the terrestrial planets accreted planetesimals and experienced an ever decreasing rate of planetary bombardment. Based on knowledge of the lunar uplands[5], this bombardment produced a thick layer of crushed silicate crust on both Mars and Earth. Some of the silicate minerals in the crust could have been converted to clays if water had been present. Evidence for the possible presence of clays on Mars, and other planets, comes from the discovery that certain classes of meteorites contain clay minerals believed to have been formed in hydrated regoliths on planetary surfaces[6]. Therefore, we believe that it is likely that clay minerals existed in the ancient soil of Mars. Comets delivered sufficient quantities of water to produce oceans on Earth similar in size to those present today. Comets impacting Mars delivered enough water to produce 10 to 100 meters of water which may have been retained for some period of time on the planet[7]. Although some of these theoretical studies suggest that liquid water may have initially covered Mars, such oceans would have been absent by 3.8 billion years ago because stream like features are present in many places by then, and many of the old impact craters are still present. The shapes of the channels suggest that small amounts of running water existed and that intermittent precipitation fed subsurface aquifers. Water from the water table came to the surface in springs at the heads of sapping channels that contained intermittent flowing water[8]. We believe that the geologic and meteorologic conditions of this environment were at least as favorable, and probably more favorable, for the origin of life as conditions that existed on Earth when life originated.

On the basis of this theoretical and empirical information, we propose the

following scenario for the chemical evolution of life on Mars: Important prebiotic organic reactants were supplied to the planet by comets, interplanetary dust, and carbonaceous chondrites. One source of evidence for this transport mechanism comes from the fact that a large object from space, believed to be a comet, caused an impact that deposited a uniform layer of clay at the Cretaceous-Tertiary boundary. Especially large amounts of amino acids have recently been discovered in association with these deposits[9]. Ultraviolet light and lightning on early Mars further provided the energy to produce photochemical reactions between CO_2 and hydrogen. Chemical compounds that could have been used for chemical evolution leading to life would have been cleansed from the atmosphere when raindrops collided with them and carried them to the surface; this process is known as "scavenging" and we know from our own experience on this planet that atmospheric chemicals become readily incorporated in rain drops. During the time that reactants were incorporated in rain drops, the simple organic compounds from space and those made in the atmosphere would have taken their first steps toward evolving into more complex polymer compounds. The development of complex, organic compounds is an important step in the chemical evolution of life.

We believe that many of these reactions would also have taken place in the crushed silicate layer present at the surface of Mars because it has been previously discovered that clay particles are very beneficial for triggering these types of polymerization reactions. The soils and deeper aquifers of Mars (comprised of this crushed silicate and clay material) would also have provided an excellent environment for the next level of chemical evolution: the formation of very complex, high molecular weight organic compounds. Solutions of simple compounds would have been moved though the soil and permeable rocks as a result of fluctuating levels of groundwater, soil leaching, capillary action, and natural percolation/filtration processes. This would have subjected compounds in the water to repeated cycles of hydration, dehydration, and redistribution on clay particle surfaces; the net result being the formation of macromolecules[10]. Over a long period of time, the crushed silicate layer acted as a large chemical processing column to form organic polymers of increasing complexity.

The next stage of chemical evolution of life took place in the bottoms of sapping channels or in the lakes that they emptied into. Ground water percolating through the crushed surface layer of rocks would have come to the surface at springs at the amphitheater heads of sapping channels. These channels are widely observed on the surface of the ancient cratered terrain of the planet. Complex polymers that were produced in the water-bearing rocks (particularly at the water table) would, at this point, have developed to cell-like structures. It has been discovered that organic polymers, when dropped into water, often form small spheres called coacervate droplets. These could represent primitive cell-like structures capable of a certain degree of independence from their environment. This would have permitted some interchange of biochemical compounds with the environment. The emergence of organic compounds from the ground into sunlight would now enable solar radiation to be utilized as an energy source to drive further chemical organization. Eventually, life may have originated in concentrated aqueous solutions at the bottoms of sapping channels or in the lakes and seas into which they discharged.

Such a model for the chemical evolution of life on Mars compares favorably with the existing model for the origin of life on Earth. Life on Earth is believed to have originated in the primordial "soup" of organic compounds in the ocean. Simple organic compounds produced in, or supplied to, the atmosphere in the same manner as that described above, settled into the ocean and became concentrated in this environment. However, on Earth, it would have taken longer for these compounds to have become concentrated because they would have initially been present in a much more dilute solution of ocean water; in the shallower water bodies initially present on Mars, solutions would have been more concentrated. The fluctuating levels of groundwater in the soil layer of Mars would also have permitted cycles of wetting and drying more efficiently than would have been possible in an oceanic environment. Repeated wetting and drying in the presence of clays promotes the development of complex organic compounds. We conclude that Mars not only provided an ideal geological environment for prebiotic chemistry, but it also provided an environment in which reactions could have occurred more rapidly than on Earth.

References: (1) Klein H. P. (1978) *Icarus* **34**, 666 (2) Maher K. A. and D. J. Stevenson (1988) *Nature* **331**, 612-614 (3) Oberbeck V. R. and G. Fogleman (1989a) Origins of Life and Evolution of the Biosphere, in press (4) Oberbeck V. R. and G. Fogleman, (1988) *LPSC* **XX**, 800 (5) Aggarwal H. R. and V. R. Oberbeck (1978), *LPSC* **IX**, 829 (6) Bunch T. E. and S. Chang (1980)*Geochim. Cosmochim. Acta* **44**, 1543 (7) Chyba C. F. (1989)*Nature*, in press, Cornell University CRSR 930 revised (8) Carr M. H. (1989) *Icarus* **79**, 311 (9) Cronin J. R. (1989) *Nature* **339**, 423 (10) Lahav N.D., D.C. White, and S. Chang (1978) *Science* **201**, 67.

SEARCH FOR LIFE: A SCIENCE RATIONALE FOR A PERMANENT BASE ON MARS, V. R. Oberbeck, NASA Ames Research Center, Moffett Field CA 94035, J. R. Marshall, Arizona State University, Tempe AZ 85287, D. E. Schwartz and R. L. Mancinelli, SETI Institute, Mountain View CA 94043

Results of the Viking mission to Mars provided no compelling evidence that extant life is present on the planet's surface. This apparent lack of evidence stems from experimental data which, at times, gave signals that could be interpreted to have been caused by organisms. But the soil samples that had been sterilized also gave the same signals. This has since been explained by probable inorganic oxidation chemistry in the surface soil[1]. Because Mars (of all of the planets in the Solar System) is the planet whose early clement history most resembles that of early Earth, it is the planet of choice on which to search for evidence of the origin of life. This remains the primary driver for further scientific exploration of Mars. The discovery of evidence for either extinct or living organisms on Mars would profoundly affect mankind because it would suggest the possibility that life may have originated in many places in the universe. Even if there were no living organisms at the Viking sites, that does not preclude the existence of life elsewhere. Most of the promising, potential Martian habitats were not explored. For example, no subsurface searches in potential water tables on Mars were made, nor were the bottoms of ancient river channels or lakes searched. Thus, we have hardly begun a proper search for evidence of past or present life on Mars. If after an extensive search we conclude that life never originated on Mars, this in itself would be a very significant finding. We would be forced to ask the question "why did life not originate on a planet so similar to ours?"

What is the basis for assuming that life may have originated on Mars? First of all, the planet was supplied with prebiotic compounds (simple chemicals that can react to eventually produce life) from comets and carbon-bearing meteorites, as was Earth. In addition, liquid water probably existed at the surface until about 3.8 billion years ago[2,3]. These are two critical requirements for life to have originated by chemical evolution. Both early Earth and early Mars were subject to intense bombardment by planetesimals and asteroids which could have, at first, prevented the origin of life. It is interesting to note that the time between large impact events was actually longer for Mars than Earth, and thus the planet had available to it longer time windows for life to originate. Consequently, there could have been sufficient time for life to originate on Mars before 3.8 billion years ago. If life existed, it may either have become extinct at the surface, leaving behind fossils, or persisted in deep groundwater after 3.8 billion years ago. This implies that evidence for live organisms should be sought beneath the surface. It further implies that evidence of extinct life should also be sought beneath the surface and in the older surface terrain, because this is the only part of the Martian surface where rocks and soils of this ancient era would be preserved.

The National Research Council (NRC) recommended searching for four types of indirect evidence for organisms on Mars[4]. These include liquid water, organic compounds, electrolytes, and biogenic gases, but the NRC points out that these are not evidence that life exists. This indirect type of evidence was among the types sought by the Viking mission. So long as chemical processes exist that generate

products which can be confused with byproducts of life, missions searching for indirect evidence of life will result in inconclusive measurements. Conclusive evidence for life cannot be sought with Viking style missions[5], nor do we believe it can be sought with other types of unmanned craft.

Considerable efforts have already been expended in deciding what types of information and instrumentation will be required to search for evidence of life on Mars. There has been a considerable discussion of the types of probes that might be used to place instruments beneath the surface of Mars where indirect measurements of the type discussed above may be made. For example, penetrators could conceivably deploy instruments that could search for this indirect evidence of life beneath the surface. Penetrators, however, can only deploy small payloads to a limited depth in a finite number of places. At best, the results obtained would only provide inconclusive evidence for life on Mars. Therefore, we believe that the search for living organisms beneath the surface will be difficult indeed. One anticipated difficulty of using a penetrator is simply that the water table might be at a greater depth than can be reached by the probe. Instead, deep bore holes may be required to reach the water table and elaborate sampling techniques may be necessary to obtain unequivocal biological samples. This type of complex and difficult task requires a human presence.

The search for fossil evidence of life at or beneath the surface will also be extremely difficult. Because the original amount of organic matter was probably small, and because there has been extensive reworking (by wind, water, and ice) and burial of original material, fossils would be scarce and difficult to find. For example, only a centimeter layer of fossiliferous material may exist in hundreds of meters of sedimentary rock. The search for such layers could be very time-consuming and would require painstaking field analysis and detailed examination, in addition to the knowledge and experience of highly trained mission specialists. Artificial intelligence techniques that could be used on unmanned surface vehicles (e.g., rovers) could be useful for preliminary, reconnaissance efforts, but during a detailed search, could easily mistake inorganic artifacts for fossil remains. It is difficult to envision how a successful search for fossils could be carried out without preliminary geological field surveys followed by exhaustive on-site laboratory investigations conducted by humans on Mars.

From an exobiological standpoint, and indeed from any scientific standpoint, the ecosystem is as important as the organisms within the system. Ecology defines the limits for the origin and continued evolution of living systems, and therefore places terrestrial ecosystems in a universal context. If organisms are discovered on Mars we must gain an understanding of the relationship of the organism to its environment in order to determine the range of environments that might harbor life in the universe. In the event that living organisms are found, they will need to be studied *in situ*. Why is this necessary? Because interrelationships between organisms and their environments are so complex, it is essential to study organisms in their natural habitat. For example, two elements that are important to organisms are nitrogen and sulfur. In terrestrial ecosystems, we know that cycling of these elements requires a community of co-existing organisms working in concert with the environment. Changing the environment leads to significant changes in the cycling.

The types of *in situ* studies that would be required to determine biogeochemical cycles in these ecosystems would be vastly compromised if they were directed from a different planet. The study of ecosystem dynamics can only be accomplished by humans inhabiting a Mars base equipped with a laboratory. The necessity for *in situ* studies is well illustrated by the hydrothermal vent ecosystem on the Earth's ocean floor. The life present in this ecosystem must be studied *in situ* because most organisms die when brought to the surface. Although they exist deep below the surface, and are difficult to study, an understanding of the ecology has warranted the use of manned submersibles.

It has recently been discovered that a large biomass of microorganisms extends to great depths within terrestrial aquifers[6]. It seems reasonable to assume that possible Martian aquifers may have been similarly colonized by microorganisms. The investigation of this ecosystem on Mars may be analogous to its investigation on Earth because of engineering problems associated with drilling and recovering pristine samples for analyses. Complex drilling and coring tasks in rugged Martian terrain can only be performed by humans operating from permanent bases that provide laboratory support facilities. Also, the careful field analysis of possible groundwater systems, required as a precursor to extensive drilling, cannot be achieved with unmanned landers. Careful drilling operations permit a portion of the environment to be brought into the laboratory (using sealed drill casings), thus enabling one to closely approximate the *in situ* environment for a short period of time before the sample deteriorates. These samples would not survive interplanetary transport to Earth laboratories.

The history of comparative planetology tells us that it is precisely the opportunity for the study of physical and chemical processes in different planetary settings that has offered completely new insights into planetary processes acting within our own terrestrial environment. The presence of humans in a permanent base on Mars will permit similar new perspectives on the importance of processes that are integral to the origin of life in a planetary context. Because the positive results of a search for conclusive evidence for past or present life on Mars would have profound implications for mankind, and because of the difficulties just discussed that are inherent in the search, we believe that this search is compelling justification for a permanent science base on Mars.

References: (1) Klein H. P. (1978) *Icarus* **34**, 666 (2) Oberbeck V. R. and G. Fogleman (1989) *LPSC* **XX,** 800 (3) Pollack J. B., J. F. Kasting, and S. M. Richardson (1987) *Icarus* **71**, 203-224 (4) Committee on Planetary Biology and Chemical Evolution, Space Sciences Board, National Academy of Sciences, 1977 (5) Hartman H., J. G. Lawless, and P. Morrison (eds.) (1985), NASA SP-477 (6) Phelps T. J., E. G. Raione, and D. C. White (1988) U. S. Dept. of Energy, DP-MS-88-100.

LARGE SCALE OBLIQUE IMPACTS ON THE EARTH ; John D. O'Keefe and Thomas J. Ahrens, Seismological Laboratory 252-21, California Institute of Technology, Pasadena CA 91125

The impact of large bodies is an important factor in the accretion of the terrestrial planets, the genesis of their atmospheres[1234] , and possibly the evolution and extinction of life. The phenomena associated with impact of large bodies on the earth with its attendant atmosphere has been numerically simulated[5 6] and measured in small scale laboratory experiments[7]. These studies were of impacts normal to the earth's surface. Here we address the more probable cases where the impact angles are oblique.

We have calculated the flow fields for normal and oblique impacts using a two-dimensional numerical computational algorithm[8]. This two-dimensional algorithm accurately models the flow field for normal angle impacts because the flow field has axial symmetry. In the case of normal impacts, the pressure and density are approximately constant across the front of the bolide, while at impact angles less than 90 °, the pressure and temperature vary exponentially with the atmospheric scale height. As for normal impacts, the shock wave in front of the bolide encounters the planet surface and reverberates between the bolide and the planet until the bolide strikes the surface and drives a radial conical shock which results in a 40 km/s radial jet of atmospheric gas emanating from the impact zone.

In the case of oblique impacts, the algorithm is an approximation to the three-dimensional flow field, most accurate in the plane normal to the planet's surface which contains the impactor trajectory. We previously used this technique to calculate the impact angles and velocities required for significant jetting and entrainment of planetary material[9].

Both the atmosphere and the planetary surface are included in the model. The atmosphere was assumed to have a scale height of 7 km. The impactor diameter is 10 km and its velocity is 20 km/s. The flow fields were calculated for impact angles ranging from 90°(normal) to 25° to the planetary surface. The flow-field resulting from passage of the impactor through the atmosphere was analytically calculated and used as the initial conditions for the numerical simulations[5]. We assumed that the bolide was incompressible during the passage through the atmosphere (Fig. 1).

The wake field behind this Mach 58 bolide was found to have a < 1° sheath travelling at 5 km/s. The front surface of the bolide was slightly flattened in a plane normal to the trajectory. A bolide with a diameter greater than the scale height, the atmosphere it encounters is trapped in front of it prior to impact. In the case of fairly oblique impacts (angles < 45°), there is not a significant amount of shock interaction prior to impact with the planetary surface and the amount of atmospheric jetting is reduced. In addition to jetting of the trapped atmosphere, there is jetting of the bolide and planet. O'Keefe and Ahrens[2] showed that at 20 km/s obvious jetting of planetary and bolide material occurs for impact angles in the range of 60 to 15°.

Preliminary flow fields for an impact angle of 25° are shown in Figs. 1 through 3. At this angle there is little jetting of the atmosphere prior to impact with the surface and most of the atmosphere is trapped in front of the bolide. The air shock pressures prior to impact in front vary from 6.9 kbars at the surface to 1.9 kbars at top of the face. As the bolide penetrates the planetary surface, the air shock is reflected from the planetary surface in front of the bolide. Subsequently, because of the interaction of the bolide and the planet, a strong jet of vaporized material followed by melt and solid material is produced. The jet and following materials propagate parallel to the planetary surface and the vapor drives a strong shock in the atmosphere (see Fig. 3). The oblique impact case differs from the normal case in that the ejecta is propelled into a quiescent atmosphere, whereas in the latter the ejecta is propelled after reflections of the atmospheric shock waves create a radial flow field that is parallel to the ejecta trajectories[5]. Because the forward jet is parallel to the planetary surface it transfers energy more effectively to the dense part of the atmosphere than normal impacts. The relative greater efficiency of oblique impact in providing sufficient energy for atmospheric escape will be discussed in detail in future work.

Oblique impacts

O'Keefe, J.D. and Ahrens, T. J.

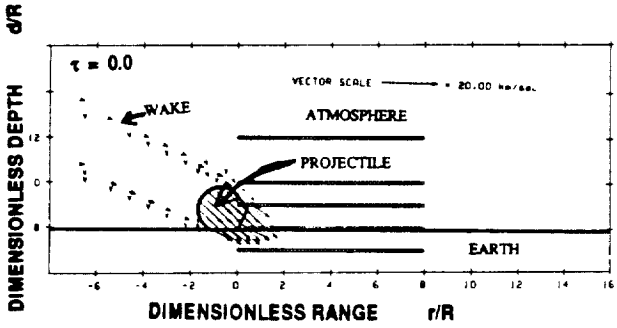

Figure 1 The atmospheric flow field at the time the impactor just hits the Earths surface.This is the initial condition for the numerical simulation shown in figures 2 and 3 The impact velocity is 20 km/s and the impact angle is 25°. The impactor radius , R , is 5 km. The horizontal line of dots in the atmosphere and earth are markers which show displacement in the subsequent flow.

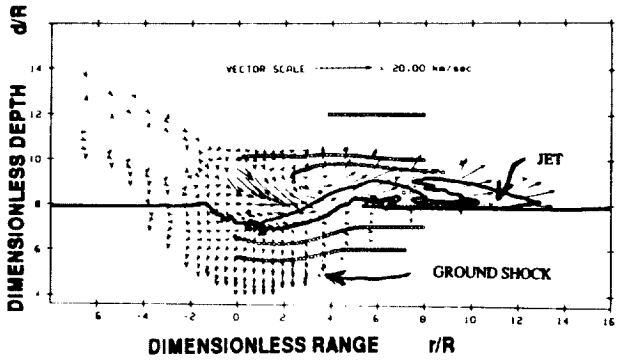

Figure 2 Flow field at dimensionless time = 6.5 (impactor diameter divided by velocity)

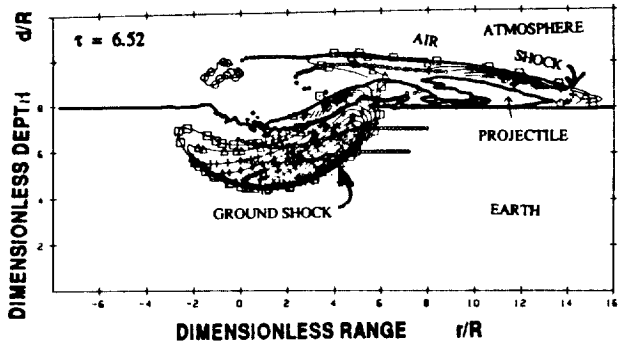

Figure 3 Pressure contours at dimensionless time = 6.5. Peak pressure in earth, projectile, and air is 137, 25, and 0.1 GPa, respectively. Contours indicate 0.005, 5, 10, 20, 30, 40, 50, 60, 75, and 90 percent of peak value.

REFERENCES

[1]Abe,Y. and T.Matsui (1985), In: Proc. Lunar Sci. Conf. 15th, part 2, J. Geophys. Res., C545-559

[2]Lange, M.A., and T.J. Ahrens (1982a), Icarus, 51, 96-120

[3]Cameron, A.G.W. (1983), Icarus, 56,195-201

[4]Wetherill, G.W., (1985), Science, 228, 877-879

[5]O'Keefe, J.D. and T.J. Ahrens (1988), Proc LPSC XIX, pg 887

[6]Roddy, D.J., S. H. Schuster, M. Rosenblatt, L.B. Grant ,P.J. Hassig, and K.N. Kreyenhagen (1987), Int. J. Impact Mechanics, 535-541

[7]Schultz P.H. and D.E. Gault (1982), Geo. Soc. Spec. Paper, 190, 152-174

[8]Thompson, S.L. (1979), SAND 77-1339, Sandia National Labs, Albuquerque,N.M.

[9]O'Keefe, J.D. and T.J. Ahrens (1986), Science, 234, 346-349

Mapping our sister planet Venus: Magellan geologic mapping mission

R. Stephen Saunders
Ellen R. Stofan
Magellan Project Office
Jet Propulsion Laboratory
California Institute of Technology
4800 Oak Grove Drive
Mail Stop 230-225
Pasadena, CA 91109
Tel. (818) 393-1001

The Magellan Mission to Venus will undertake the ambitious task next year of mapping our sister planet, Venus. Venus, is nearly the same size as Earth, and since it has no oceans, the surface area is nearly four times the land area of our planet. The Magellan science team hopes to learn why Venus evolved so differently from Earth, with its surface temperature hot enough to melt lead and its thick carbon dioxide atmosphere.

Magellan will arrive at Venus on 10 August 1990 and begin radar mapping of Venus about 1 September. A radar imaging system, called synthetic aperture radar, is needed to see the surface through the thick, cloudy atmosphere. The resulting images, however can be interpreted in much the same way as aerial photographs or spaceborne television images. The objective of the mission is to map the planet at a resolution of 120 m to 360 m resolution (400 to 1200 feet). The spacecraft, controlled from the Jet Propulsion Laboratory, will be placed in a 3.1 hour, near polar orbit. On each orbital revolution Magellan will map a strip of Venus about 25 km wide (16 miles) and 17,000 km long (10,000 miles). In this way, nearly 90% of the surface can be mapped in the 243 day mission, equal to one Venus day.

A global geologic map of Venus will be produced at a scale of 1:15 million. This map will be compiled from many individual geologic maps using mosaicked images in the form of prints at a scale of 1:2 million. Topical maps will also be produced at the same scales to show the distribution of impact craters, volcanic flows, mountainous ridge belts, faults and other tectonic features, the mysterious coronae seen in the Soviet Venera radar images, and other geologic features. Special maps for geophysical analysis, including gravity, topography, surface radar properties, and microwave emission, will also be constructed.

Since Venus is so large compared to the other planets the task of producing even a preliminary map of Venus is enormous. The Magellan spacecraft will return as much image data as all of the NASA planetary imaging missions to date. This large amount of data requires the use of new technologies, such as compact disks (CD-ROM) for data distribution.

The Magellan spacecraft, launched from the Space Shuttle

Atlantis on May 4, 1989, will arrive at Venus on August 10, 1990 after its 462 day trip from the Earth. The data it collects will represent nearly three times improvement in coverage and ten times improvement in resolution over previous data of Venus. The longitude of arrival at Venus is about 276 degrees East, and Venus turns beneath the orbit track 1.48 degrees per day. An In-Orbit-Checkout (IOC) period of 21 days is planned before the start of mapping. During IOC some imaging is planned as early as Day 6 (August 16) (about 286 deg. longitude). Multiple mapping swaths are planned for day 12 and some image data may be obtained on Day 17, as part of tests of the radar. Mapping will start on Day 21 (August 30, 1990), with the caveat that the best parameters for operating the radar may not yet have been determined. During the first few weeks of the mission, major questions about the geology of Venus will be answered as many different types of features and terrain are imaged. In addition, many new questions will be raised as discoveries are made.

During IOC radar tests, a range of types of features may be imaged:

DAY 6 - Eastern Beta Regio and Devana Chasma
Golubkina and Lagerlof Craters
DAY 12 - Brooke Crater
Atropos and Lachesis Tessera
Demeter and Pomona Coronae
Tefnut Mons
DAY 17 - Dashkova and Ivka Craters
Otau Corona
Venera 13 landing site

In spite of its thick atmosphere (90 times as thick as Earth's), Venus appears to have impact craters. In some ways we might expect Venus craters to resemble those that could form on the floor of shallow seas on Earth. The impact craters that Magellan will image early in the mission are of differing size and degree of preservation; for example, Golubkina is a 28 km diameter relatively fresh bright halo crater while Dashkova is a 48 km across eroded crater. What processes are causing the erosion of surface features? Faults associated with a major rift zone (Devana Chasma) in Beta Regio will be covered on Day 6. The rift in Beta has been compared to the East African rift (1), and will enable us to learn more about how rifting operates on the Earth as well as Venus.

Several types of features discovered by the Soviet Venera 15/16 spacecraft in 1984 will be imaged during IOC including tessera (complexly deformed highland regions) and coronae (170-690 km across circular structures) (2). Both of these may form by processes operating on the Earth, but may have been extensively modified under Venus conditions. Coronae may form over hot spots, similar to Hawaii. On Venus, temperatures are so high that rock can behave more like a fluid (3, 4). High topography associated with features such as coronae may 'flow' away in the geologically short time of about 100 million years (much less than the 1.0 billion year age of the surface

determined with previous data (5)) (6). The tessera terrain also may have undergone this process, called gravitational relaxation (7). Head (8) has compared the morphology of the tessera terrain to the Earth's seafloor. This analogy can be more fully tested as Magellan sends back high resolution images and altimetry of several different tessera regions during the first weeks of mapping by Magellan. Also covered during IOC is the landing site of the Soviet Venera 13 spacecraft. The lander sent back images of a surface covered with soil and platy rocks of basaltic composition (9). Magellan will provide the link between the ground truth obtained by the lander and lower resolution global data sets such as Pioneer Venus.

DAY 21- Nominal start of mapping

The planned start of mapping occurs at the western edge of Ishtar Terra. The radar will map from 80 deg. N to about 67 deg. S. Ishtar Terra is a region of topographically high folded and faulted mountain belts (10). Akna Montes will be mapped from Day 21-33, Freyja Montes from about Day 29 until about Day 53. The northern boundary of Ishtar is characterized by highly deformed terrain (Itzpapalotl Tessera- starting Day 21) indicating a great deal of compressional deformation and 'piling up' of material (11). The southern boundary of Ishtar is characterized by a mountain belts (Danu Montes) and two steep scarps (Ut and Vesta Rupes) of unknown origin. This area will be mapped from about Day 25 on.

Magellan will also provide the first comprehensive high resolution data of the southern hemisphere of Venus, including data over regions of unknown origin such as Themis Regio, Phoebe Regio, Alpha Regio and northern Lada Terra. Phoebe and Alpha show some characteristics similar to tessera (12). Crustal spreading/plate tectonics models (13) predict that a great deal of compressional deformation should be found at low latitudes in the southern hemisphere. Magellan will provide the answers to these controversies.

Is there active volcanism on Venus? What can the range of volcanic features observed tell us about questions such as the amount and the composition of materials erupted onto the surface? Many different types of volcanic features will be imaged in the first few weeks, from huge caldera structures to 10 km across domes to systems of volcanic flows 100's of kms long. In the center of Ishtar Terra lies a high plateau (Lakshmi Planum) with two very large (> 150 km across) volcanic calderas (Colette and Sacajawea). In the Venera 15/16 data, systems of flows can be seen around Colette (2, 14). Why are these calderas so elongate and so deep? Additional, abundant volcanic features have been imaged by Earth-based radar in the plains south of Ishtar, including long radar-bright and dark flows and domes (15). The order of magnitude better resolution of Magellan should enable us to identify the sources of many of the flows, their age, and how they erupted. Hathor, Innini and Ushas Mons in the southern hemisphere will be mapped from about Day 27 to 33. These features are large (>1.5 km high, >250 km across) volcanic

shields which may be similar to plume-swell type volcanoes seen at Hawaii.

A variety of other features will be covered in the first few weeks of mapping. Many craters will be imaged, including the multiple ring structure Meitner (84 km across) (Day 22) and the 'crater farm' (a close grouping of craters in the southern hemisphere) (Day 37). Magellan will aid in determining the impact or volcanic origin of these features. In addition, two Venera landing sites will be imaged. The Venera 14 landing site will be imaged on Day 21. Images of this landing site show a surface covered with platy rocks of basaltic composition (9), similar to surfaces one might see in Hawaii (16). The Venera 8 site will be encountered on about Day 39, and appears to be underlain by rocks of granitic composition from lander elemental analyses (17). Could this be a region of ancient crust or exposed, highly evolved rocks?

One of the most important problems that Magellan will address will be a more accurate determination of the age of the surface. Venera 15/16 data indicate that the age of the surface is older than that of the Earth as mentioned above, but some estimates put the age much closer to that of the Earth's surface (18). The other terrestrial planets (Mars and Mercury) and the Moon have very old surfaces (about 3 billion years since any major geologic activity). These bodies are all small, while Venus is about the same size as the Earth. Many scientists believe that the size of a planet determines the nature and duration of geologic activity on the surface. A large planet such as the Earth has more internal heat-producing elements which drive geologic processes and thus a relatively young surface. Is Venus really more like the Earth? Does it have active processes such as hot spot volcanism and plate tectonics? Some believe that Venus may provide a 'window' into the Earth's past- to a time when the process of plate tectonics was just beginning or had not yet begun. Magellan will provide us with a better idea of the surface age, as well as a better understanding of the origin of features glimpsed in earlier data sets of the planet.

REFERENCES 1) G.E. McGill et al., GRL, **8**, 737, 1981. ; 2) V.L. Barsukov et al., JGR, **91**, 378, 1986.; 3) J. Weertman, Phys. Earth Planet. Int., **19**, 197, 1979.; 4) S.C. Solomon et al., JGR, **87**, 7763, 1982.; 5) B.A. Ivanov et al., JGR, **91**, 413, 1986.; 6) E.R. Stofan et al., submitted, JGR, 1990; 7) D.L. Bindschadler and J.W. Head, submitted, JGR, 1990; 8) J.W. Head, LPSC XX, 394, 1989.; 9) Y.A. Surkov et al., Proc. LPSC 14, JGR, **89**, 393, 1984.; 10) L.S. Crumpler et al., Geology, **14**, 1031, 1987.; 11) J.W. Head, LPSC XIX, 467, 1988.; 12) D.L. Bindschadler et al., in press, GRL, 1990. 13) J.W. Head and L.S. Crumpler, Science, **238**, 1380, 1987. 14) K.M. Roberts and J.W. Head, LPSC XX, 910, 1989.; 15) D.B. Campbell et al., Science, **246**, 373, 1989.; 16) J.B. Garvin et al., JGR, **89**, 3381, 1984. 17) A.P. Vinogradov et al., Icarus, **20**, 253, 1973.; 18) G.G. Schaber et al., LPSC XVIII, 874, 1987.

DECAPITATED IMPACTORS IN THE LABORATORY AND ON THE PLANETS; P.H. Schultz, Brown University, Providence, RI 02912 and D.E. Gault, Murphys Center of Planetology, Murphys, CA 95247.

Background: The partitioning of energy during oblique impacts is very different from vertical impacts. For vertical impacts into sand, about 73% of the initial impactor energy is expended in target displacement including 20% in compaction and 53% in ejecta (1). The remaining energy (27%) is partitioned into waste heat and kinetic energy of the projectile. At low impact angles (15° from the horizontal), however, most of the impactor energy occurs as kinetic energy in ricocheted debris (2, 3). Internal energy in the projectile decreases as $\sin^2\theta$ until ricocheting nearly intact at very low impact angles (<7.5°), even at hypervelocities (>6 km/s) into non-porous targets (3). Oblique impacts of ductile aluminum into solid aluminum targets have been observed to consistently produce nearby downrange pits (2, 4). Because these enigmatic pits occur within a few projectile diameters of first contact, they cannot be caused by hypervelocity ballistic ejecta from the target. They appeared to be produced instead by decapitation of the projectile due to spallation.

Laboratory Experiments: Positioning the target edge close to the expected downrange rim of the primary crater permitted isolating the downrange impacting fragments from the first impact. Vertical witness plates placed farther downrange recorded the dispersion and trajectories of these isolated fragments. High-frame rate imaging from 35,000 fps to 2 x 10^6 fps (frames per second) constrained their velocity within about 5% and permitted deriving the size of the fragments from the size of the impact pits through scaling relations for identical materials (5). Aluminum and pyrex spheres (0.635 cm spheres) were launched at hypervelocities (~5 km/s) in order to contrast the response of ductile and brittle materials. Aluminum targets included a range of thicknesses (from 0.079 to 2.5 cm) in order to explore first-order effects of initial contact. Different targets (soft aluminum, sand, and water) were also used to calibrate compositional effects.

High velocity impact (5–6 km/s) of 0.635 cm aluminum spheres into 2.5 cm thick aluminum targets produce a characteristic ricochet pattern with a horizontal concentration and vertical strings of more isolated impact pits. Isolation of the downrange second impacts, however, produced only a faint horizontal line of very small pits. In such cases, the largest pits occurred well below the impact surface plane and only slightly (but significantly) above the projected intercept of the original impactor trajectory. For thin targets (less than 0.5 projectile diameter), the observed vertical offset depended more on proximity to the target edge than on target composition or thickness. The vertical offset resulting from impacts into thick aluminum targets typically correspond to a 10° change from the original trajectory. High frame-rate photography revealed that the velocity of the fragments were indistinguishable from the launch velocity, i.e., a loss of no more than 300 m/s. This record also clearly distinguished the high-speed (9 km/s) jetting component from a lower speed (~3 km/s) cloud of expanding self-luminous ejecta directed along the impact plane. The latter component was observed to uniformally plate the witness plate and pits with a microscopically thin layer of aluminum.

Discussion: The laboratory experiments clearly demonstrated that the downrange ricochet pits indeed result from spallation of the top of the projectile. At a 15° impact angle, decapitation produces a bimodal distribution with 4 to 8 fragments of nearly equal size and numerous smaller debris. Because these fragments did not impact the target surface, larger fragments survive (Figure 1). The small near-vertical velocity component of the spalled debris is generally consistent with calculated peak pressures based on the approach of Gault and Heitowit (6) modified to include only the vertical velocity component. For 5 km/s impact velocities, the shock created by first contact reaches the top of the projectile before it has penetrated 10% of its diameter into the surface. Even brittle and fragile pyrex spheres exhibited surviving fragments 10–20% of the original projectile diameter at 5.4 km/s and 15°. We note that oblique impacts into easily volatized targets (plasticene, water, carbonates) in addition produce a significant boost to the spall velocity, most likely due to acceleration in the observed impact-generated vapor cloud (7).

Hence, internal energy losses in the projectile appear to decrease for oblique impacts owing to spallation of the free surface. Several observations suggest, however, that internal energy losses along the projectile/target interface increase. First, the photographic records reveal a self-luminous ejecta cloud separable from the jetting phase that expands non-ballistically—even below the target reference surface. Second, aluminizing of thin pyrex witness plates placed just 2.5 cm above the impact indicate considerable internal but little kinetic energy in the expanding ejecta cloud. And third, downrange discoloration of the target occurs within a broad parabolic-shaped fan. This discoloration suggests brief but intense heating related to ejecta, not target-transmitted shock heating. Hence, the decrease in projectile fragmentation with decreasing impact angle down to 15° is paradoxically accompanied by an increase in heating, even for impacts into aluminum where calculated peak shock pressures are sufficient to induce only partial melting (1). This heating is expressed not only by jetting but also by fine incandescent (perhaps even melted and vaporized) aluminum ejecta. We attribute such heating to mechanical shear, a process commonly used to weld dissimilar materials, and we suspect that internal losses by shear heating may exceed shock-induced losses for impact angles less than 20–30°.

The downrange patterns resulting from projectile spallation observed in the laboratory have

DECAPITATED IMPACTORS
P.H. Schultz and D.E. Gault

striking analogs in the planetary record. Re-examination of the oblique impact record on the Moon and Mars reveals numerous examples of downrange re-impacts. The specific pattern depends on local topography and crater size. On flat surfaces, nearby and downrange oblique impact are readily recognized (Fig. 2a). At low impact angles, however, local slopes can significantly affect not only the distance between first and ricochet impact but also can change the impact angle of decapitation fragments. Ricochet from oblique impacts on the floors of several large martian craters exhibit re-impact craters on the facing wall that are even larger than the crater resulting from the initial impact. In contrast, downslope collisions have produced a succession of smaller, shallower impacts (Fig. 2b). At the broadest scales, the initial impact and downrange re-impact merge. Orcus Patera (450 km x 150 km) on Mars exhibits the diagnostic ejecta pattern for an oblique impact and a series of smaller coalescing impacts downrange. The crater Schiller on the Moon is accompanied by a series of larger downrange, coalescing craters due to the topographic effects of the facing wall/ring of Schiller basin. Both morphologies can be understood in terms of the processes observed in the laboratory. Although it can be argued that such (or some) companion impacts reflect multiple impacts by tidally disrupted or binary asteroids, the consistent pattern of smaller/shallower impacts downrange on flat surfaces, the sequence of impact, and the observed controlling effects of topography all support a process analogous to projectile decapitation observed in the laboratory.

Concluding Remarks: Laboratory experiments reveal fundamental differences in the partitioning of energy with impact angle and can be supported by both first-order theoretical considerations and planetary analogs. We feel that the process and observed phenomena provide more than just an explanation for enigmatic or unique impact structures. The decreased disruption and ricochet of a single basin-forming impactor at low angles (<15°) could contribute significantly to a sibling population of impactors, particularly in satellite systems (see 8). The increased partitioning of energy into shear heating at more modest angles (10-30°) could affect the formation and recycling of planetary atmospheres (9). Finally, the combination of vapor release and embedded projectile ricochet provides a mechanism for episodically creating orbiting debris around solid-surface planets that could evolve into a short-lived ring (3, 10).

References: (1) Braslau, D. (1970) *J. Geophys. Res.* 75, 3987-3999. (2) Gault, D.E. and Wedekind, J. (1978) *Proc. Lunar Planet. Sci. Conf. 9th*, 3843-3875. (3) Schultz, P.H. and Gault, D.E. (1990) In *Proc. of Catastrophes in Earth History*, *Geol. Soc. Sp. Paper* (in press). (4) Summers, J.L. (1959) NASA TND-94. (5) Denardo, B.P. *et al.* (1967) *NASA TND-4067*. (6) Gault, D.E. and Heitowit, E.D. (1963) *Proc. Sixth Hypervelocity Impact Symp. Vol. 2*, 419-456. (7) Schultz, P.H. (1988) In *Lunar and Planet. Sci. XIX*, LPI, Houston, 1039-1040. (8) Hafen, C. *et al.* (1990) In *Lunar and Planet. Sci. XXI*, LPI, Houston (this volume). (9) Schultz, P.H. (1988) *Eos* 69, p. 386. (10) Schultz, P.H. *et al.* (1990) In *Lunar and Planet. Sci. XXI*, LPI, Houston (this volume).

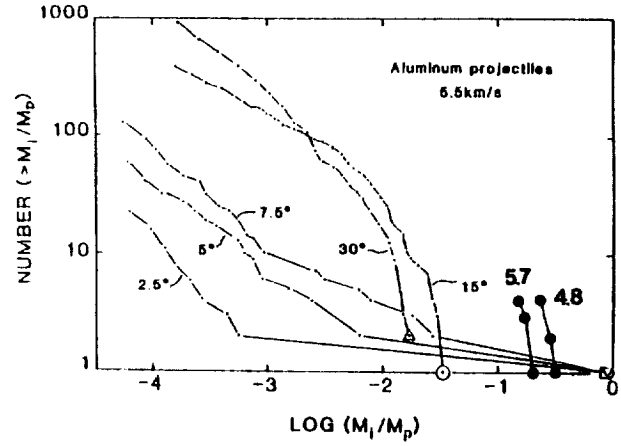

Figure 1. Size distribution of ricocheting projectile resulting from oblique impacts (referenced to horizontal) of sand (dots) and 2.5 cm-thick aluminum (large filled circles) targets. For impacts into aluminum targets, the ricochet component was prevented from re-impacting the target surface, thereby preserving the actual size and trajectory of the spalled projectile. Only the four largest spall fragments are shown for two different velocities.

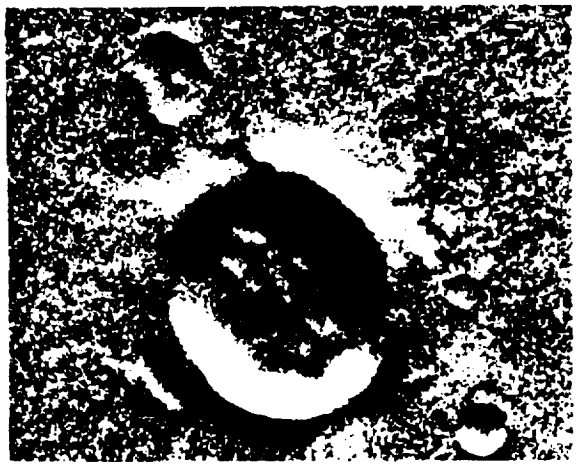

Figure 2a. Numerous craters on Mars exhibit evidence for downrange impact by spall fragments from the top of the projectile. Figure 2a shows a 4.2 x 5.5 km diameter crater with companion downrange impact (387B06).

Figure 2b. Illustrates a 15 x 35 km-diameter crater that impacted the downsloping wall of Kasai Vallis (519A27). Although appearing to be the consequence of multiple impacts, the same pattern can be reproduced in the laboratory by successive spallation and impact of a single projectile.

EARTH-CROSSING ASTEROIDS, 1989; E.M. Shoemaker, C.S. Shoemaker, R.F. Wolfe, and H.E. Holt, U.S. Geological Survey, Flagstaff, AZ 86001.

The year 1989 marked a high point in the discovery of Earth-crossing asteroids. Thirteen new Earth crossers were found during the year, five of them in one remarkable dark-of-the-Moon observing period in late October and early November. These new discoveries increase the total of known Earth crossers to 96, including 9 Atens, 61 Apollos, and 26 Earth-crossing Amors. Of these asteroids, 59 have precisely determined orbits and are now numbered, 10 are lost, and most of the remainder have been discovered too recently to have been observed on a second apparition.

Two discoveries in 1989 of special interest were 1989 AC and 1989 FC. Found on January 4 by J.-L. Heudier, R. Chemin, A. Maury, and C. Pollas at Caussols, France, 1989 AC is the sixth brightest known Earth crosser (H = 14.2). It was followed at about 20 observatories around the world. An early preliminary orbit permitted C.S. Shoemaker to find and measure prediscovery positions from films taken by H.R. Holt and T.A. Rodriquez at Palomar on July 17, 1988. This increase in the length of the observed arc enabled C.M. Bardwell to link 1989 AC with 1934 CT, which was observed on two nights in February, 1934, at Uccle, Belgium. Hence, 1989 AC was actually the second Apollo asteroid to be observed at the telescope.

1989 FC was discovered at Palomar by H.E. Holt and N.G. Thomas on March 31, 1989, eight days after it had passed within about 690,000 km of the Earth. This is the closest known approach of any asteroid to Earth. A campaign of observations organized by E. Bowell of Lowell Observatory resulted in a good preliminary orbit based on a 66-day arc; this orbit should be sufficient to permit recovery observations of 1989 FC in 1990, which are needed to assure that this very faint object will not be lost. At H = 21.0, 1989 FC and 1988 TA are the faintest known asteroids with relatively accurate orbits. If they are S-type asteroids, as are the majority of known Earth crossers, they are about 200 m in diameter.

Our estimate of the population of Earth-crossing asteroids to H = 17.7, based on discoveries to date, is as follows:

	Number Discovered ($H \leq 17.7$)	Percent Discovered	Estimated Population ($H \leq 17.7$)
Atens	5	(5.8)	90 ± 40
Apollos	40	5.8	690 ± 300
Earth-crossing Amors	15	(5.8)	260 ± 130
Total Earth crossers	60	5.8	1040 ± 470

The total population is based on the rate of discovery of Apollos with the 46-cm Schmidt camera at Palomar Observatory, and the proportions of Atens, Apollos, and Earth-crossing Amors is based on their proportions among the discovered objects. Present evidence suggests that the discovery of Earth-crossing asteroids is complete at H = 13.24, the magnitude of the brightest known object. For Earth crossers fainter than mag 15.8, the slope of the magnitude-frequency distribution is assumed to be similar to that of main-belt asteroids (cumulative frequency approximately proportional to $e^{0.92H}$), as shown in Fig. 1. The frequency evidently drops precipitously for objects brighter than mag 15.8 (cumulative frequency roughly proportional to e^{2H}).

A check on the inferred magnitude-frequency distribution of the Earth-crossing asteroids is provided by the frequency with which Earth crossers have been accidently rediscovered. About 8 have been rediscovered or recovered without deliberate search. Examples are (1627) Ivar, (2100) Ra-Shalom, (2201) Oljato, (3573) 1986 TO, (4179) 1989 AC, and (4183) 1959 LM, all of which were lost after their first detection. The accidentally rediscovered asteroids are all brighter than H = 16.25; most are mag 15 or brighter. The number of discovered objects brighter than mag 16.25 is 37; the fraction of rediscoveries (6/37) suggests that discovery is about 16% complete and that the population is about $37/0.16 \approx 230$ to mag 16.25. This number is close to the estimate of 270 indicated by the dashed line in Fig. 1. At H = 15.0, 4 out of 12 known objects have been accidentally rediscovered, which suggests that completeness of discovery at this magnitude is about 33%; the completeness indicated in Fig. 1 is 35%. The brightest Earth crosser, (1627) Ivar, was discovered in 1929, then lost, rediscovered in 1957, and serendipitously recovered in 1985 with the Palomar 46-cm Schmidt. Another Earth-crossing asteroid as bright as or brighter than Ivar is unlikely to have escaped detection.

We have updated our estimates of probabilities of collision with the Earth for Earth-crossing asteroids, using the equations of Shoemaker et al. [1]. Where we were unable to derive the collision parameters from secular perturbation theory, we used the equations of Opik [2]. The frequency distribution of collision probabilities is strongly skewed (Fig. 2): half a dozen asteroids have collision probabilities substantially

exceeding 10^{-8} yr^{-1}. Mean probability of collision is 10.7 x 10^{-9} yr^{-1} for Atens, 4.1 x 10^{-9} yr^{-1} for Apollos, and 1.4 x 10^{-9} yr^{-1} for Earth-crossing Amors. The grand mean probability of collision obtained for all categories of Earth-crossing asteroids is 4.2 x 10^{-9} yr^{-1}. The uncertainty in this estimate probably is about 40%.

Multiplying the mean collision probability by the estimated population at H = 17.7, we estimated the present rate of collision for Earth-crossing asteroids to be (4.3 ± 2.6) x 10^{-6} yr^{-1}, about 30% higher than that reported by Shoemaker et al. [1]. The colliding flux consists of about 65% Apollos, 25% Atens, and 10% Amors. Using improved data on the proportion of S- and C-type asteroids and the rms impact speed, weighted according to collision probability, of 17.9 km s^{-1}, we estimate that the production rate of asteroid impact craters larger than 10 km in diameter is (1.4 ± 0.7) x 10^{-14} km^{-2} yr^{-1}, somewhat lower than that given by Shoemaker et al. [1] and Shoemaker [3]. The collision rate of Earth crossers to H = 15.8 (roughly equivalent to S-type asteroids with diameters greater than 2 km) is about 7 x 10^{-7} yr^{-1}; the rate to H = 13 (asteroids roughly 9 km in diameter and larger) is about 3 x 10^{-9} yr^{-1}.

References: [1]Shoemaker, E.M., Williams, J.G., Helin, E.F., and Wolfe, R.F., 1979 in Gehrels, T., ed., Asteroids, Tucson, Univ. Arizona Press, p.253-282. [2]Opik, E.M., 1951, Proc. Roy. Irish Acad. 54A, p. 165-199. [3]Shoemaker, E.M., 1983, Ann. Rev. Earth Planet. Sci., v. 11, p. 461-494.

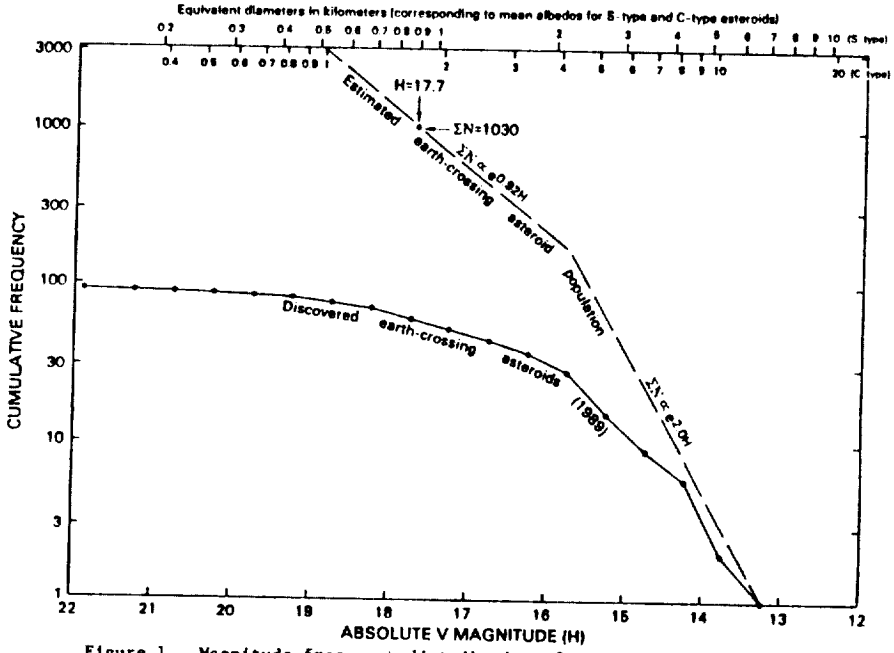

Figure 1. Magnitude-frequency distribution of Earth-crossing asteroids

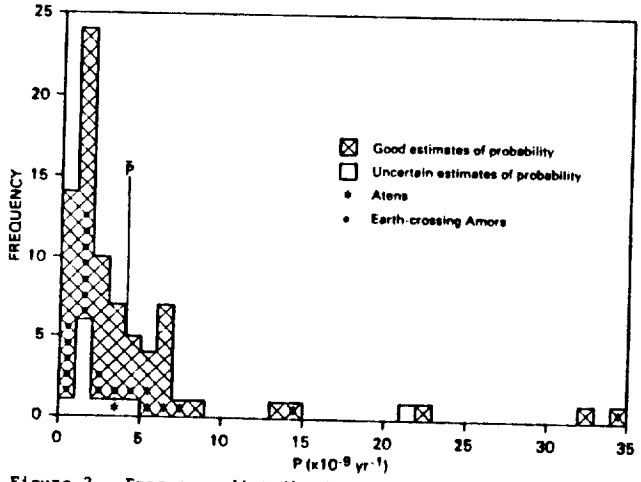

Figure 2. Frequency distribution of probabilities of collision with Earth for Earth-crossing asteroids

DISK-RESOLVED GROUND BASED INFRARED IMAGING OF IO; J.R. Spencer, M.A. Shure, M.E. Ressler, D. Toomey, A. DeNault, W.M. Sinton, University of Hawaii; J.D. Goguen, Jet Propulsion Lab.

Abstract for Press Use

We have used a new infrared camera at the NASA Infrared Telescope Facility to obtain the first detailed images taken from the Earth of the thermal radiation from the volcanos of Jupiter's active moon Io. The images reveal the existence of a previously unknown volcano and demonstrate a powerful new tool for the study of one of the solar system's most fascinating bodies.

Io is the innermost of Jupiter's four large moons. It is similar in size and density to our own Moon but utterly different in its geology. Its shape is distorted by the tides of Jupiter, and perturbations to its orbit by the gravity of its neighboring satellites cause constant flexing of this tidal bulge. As a result, enormous quantities of frictional heat are produced within Io, partially melting its interior. The heat escapes in the form of furious volcanic activity, discovered by the Voyager 1 spacecraft in 1979.

The heat radiation of Io's volcanos is readily detected by telescopes on Earth, and has been used to monitor the volcanic activity in the eleven years since the Voyager flyby. However, from Earth the disk of Io is never larger than 1.2 arcseconds, about the size of a dime seen from two miles away. Because of interference from the Earth's atmosphere even the largest telescopes on Earth can rarely see details smaller than one arcsecond in size, so Io normally appears as a fuzzy dot of light with virtually no surface details visible. Also, almost all the radiation from Io's volcanos is in the infrared, at wavelengths longer than 3 microns (visible light has wavelengths between 0.4 and 0.7 microns). Until recently cameras sensitive to the appropriate infrared wavelengths have not been available, and astronomers have had to observe Io with instruments that simply measured the total infrared radiation from the satellite, and did not produce an image.

So while detection of Io's volcanos from Earth is straightforward, astronomers have relied on indirect techniques to distinguish individual sources and find their positions on the surface. These have included using very short exposures to freeze the blurring of the Earth's atmosphere, measuring the polarization of the heat radiation, or taking advantage of the very rare occasions when another moon passes in front of Io and blocks the radiation from each volcano in turn. Normally, only one discrete volcanic source is detected unambiguously by these techniques, the massive volcano Loki, which completely dominates the volcanic radiation from the hemisphere of Io where it occurs. In 1979, the close-up Voyager observations found many smaller volcanos in addition to Loki, but there has been little chance since then to monitor the progress of these smaller features.

Recently, infrared cameras have been developed that are sensitive to radiation with wavelengths from 1 to 5 microns and are thus capable of detecting Io's volcanos. In 1989 the nation's premier center for planetary infrared astronomy, the NASA Infrared Telescope Facility at Mauna Kea Observatory in Hawaii, developed such a camera, called ProtoCAM. The development team included Mark Shure, Mike Ressler, Doug Toomey, and Tony Denault. On the nights of 21–23 December 1989 Shure, Ressler, and John Spencer, following suggestions by Jay Goguen and an observing proposal by Spencer, used the camera to take pictures of Io at various places in its 1.77-day orbit around Jupiter. On the night of 23 December they made a continuous movie at a wavelength of 3.8 microns, with frames every 3.5 seconds, of the eclipse of Io by Jupiter's shadow and its subsequent disappearance behind Jupiter. Normally the glow of the volcanos must be seen against a background of reflected sunlight from the disk of Io, but during eclipse only the volcanic radiation is visible, allowing more sensitive measurements of the volcanos. Two hours later, they made a similar movie of the re-emergence of Io from behind Jupiter.

On all three nights, the smallest features visible were a remarkable 0.4 arcseconds across. As a result, details are easily seen on Io's 1.2 arcsecond disk. The excellent sharpness was probably due to a combination of the good qualities of the 13,500 foot elevation Mauna Kea site, good weather conditions, and the fact that infrared radiation is distorted less by the Earth's atmosphere than visible light. The images provide a

dramatic demonstration of our ability to take much sharper pictures of the heavens from the Earth's surface than was thought possible till recently.

Images taken before eclipse by Jupiter show Io's disk illuminated by sunlight, with the glow of the massive volcano Loki visible as an off-center bright spot (Fig. a). A single image like this allows determination of the position of Loki on Io to an accuracy of 10–20 degrees in latitude and longitude: preliminary measurements indicate a position consistent with those measured by the indirect techniques mentioned above.

As Io entered eclipse by Jupiter, the edge of Jupiter's shadow could be seen sweeping across Io's disk (Fig. b), progressively cutting off the sunlight until only the glow of the volcanos was visible. Fig. c shows Io shortly after complete entry into Jupiter's shadow. Computer processing has been used to brighten the features in the image, so that the glow of the major volcano Loki is highly overexposed. The complex cross-like shape of the image is due to minute imperfections in the telescope optics, visible because of the exceptional sharpness of the picture. On the left is the edge of Jupiter's disk, which is very dark because of the absorption of this wavelength by methane in Jupiter's atmosphere. In about the 8 o'clock position from Loki, half-way to the edge of Jupiter, is the faint glow of a second, previously unknown volcano. This volcano is only 0.9 arcseconds distant from Loki and about 20 times fainter, comparable in brightness to some of the smaller volcanos detected by Voyager. Its position with respect to Loki places it on the other side of the disk, in a region seen close-up by Voyager in 1979, though Voyager did not detect any volcanic radiation from this region.

Shortly after the image in Fig. c was taken, the new volcano disappeared behind the edge of Jupiter. Fig. d shows Loki alone, after the disappearance of the new volcano. About two minutes later, Loki itself disappeared. When Io reappeared on the other side of Jupiter two hours later, it was in full sunlight and the new volcano was invisible against the sunlit disk, but the reappearance of Loki was easily seen. Because the position of the edge of Jupiter and the orbit of Io are precisely known, the disappearance and reappearance times of the volcanos can be used to place them quite accurately on the surface of Io, and this work is now in progress.

These observations are important not only because they have discovered a new volcano on Io, but because they provide a new way of finding and studying Io volcanos. The new volcano and others like it can be seen during every eclipse of Io, providing up to 75 minutes of observations several times a month from any one place on Earth for the eight months of every year when Jupiter is favorably placed in the sky. By taking images at a variety of wavelengths we can determine their sizes and temperatures, thus providing clues as to the materials involved. There is a long-standing controversy over the relative importance of sulfur and silicate (ordinary rock) volcanism on Io, and because molten silicates can attain much higher temperatures than molten sulfur, the presence of even small areas at temperatures above about 800°K (1000°F) is strong evidence for the presence of silicates.

We can determine the positions of the volcanos on Io from their locations in the images or, more accurately, by timing disappearances and reappearances behind Jupiter, and by making observations over periods of months or years we can learn the history of individual features. We can thus learn the lifetimes of the volcanos and tell whether certain areas are more prone to volcanic activity than others. All these observations will help us understand the processes driving Io's activity, and give us a much more complete picture than previously possible of this remarkable satellite. The observations will also be of great importance for the support of future space missions such as the Galileo Jupiter orbiter, allowing us to place the close-up observations in a longer-term perspective and to aim the spacecraft instruments at the most interesting areas on Io.

Figure Captions

Figure a. Infrared image of Io before eclipse, showing the sunlit disk and the thermal radiation from the major volcano Loki (upper right).

Figure b. Io entering eclipse by Jupiter's. Jupiter's shadow has covered the left (western) hemisphere, while Loki is still in sunlight.

Figure c. Io in eclipse by Jupiter, showing the glow of the volcano Loki (overexposed) and a new volcano, discovered on these images, to the lower left of Loki. See text for details.

Figure d. Io partially hidden behind the edge of Jupiter. Loki is still fully visible but the new volcano is now hidden by Jupiter.

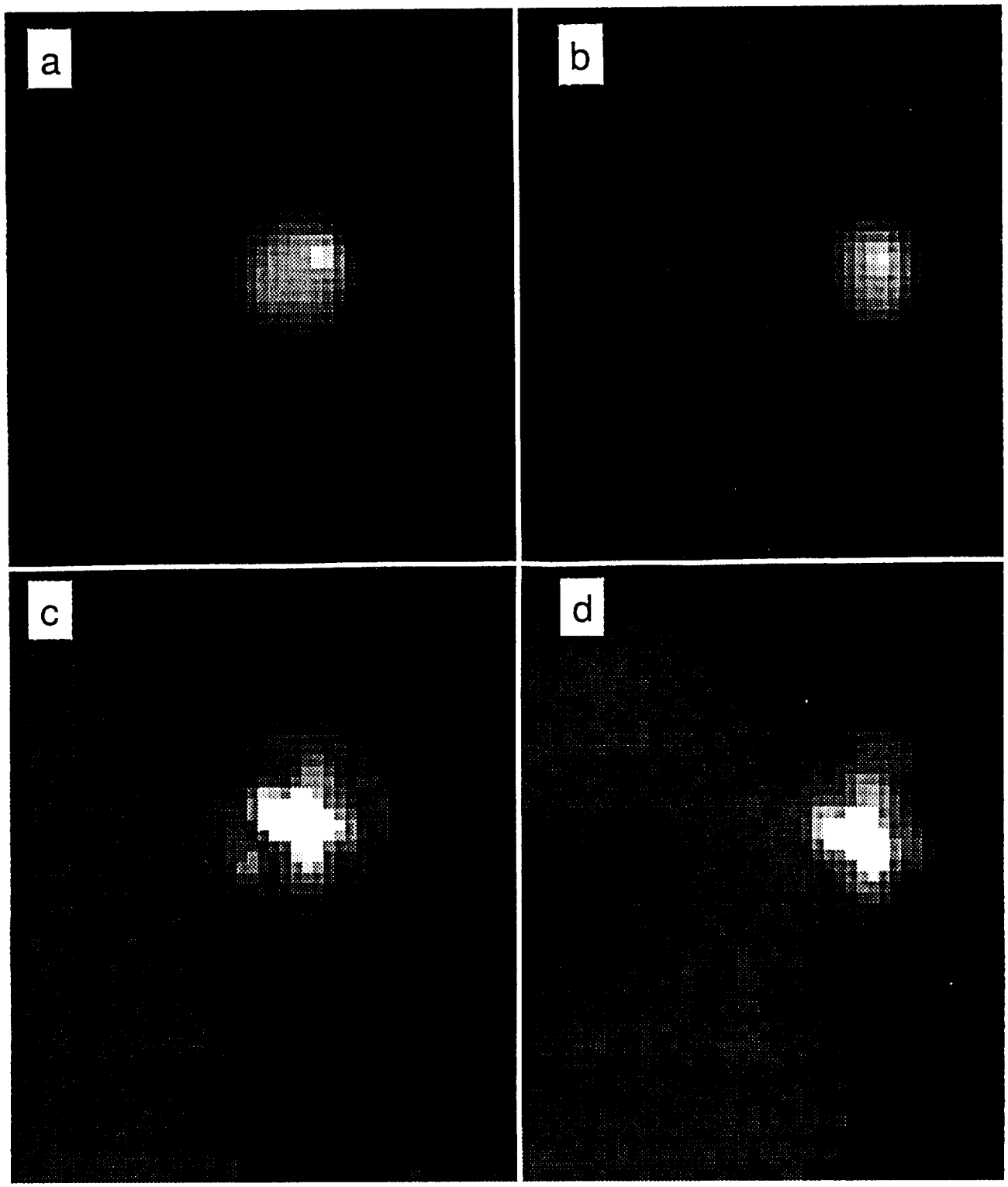

DRY CARBONATE FORMATION ON MARS: A PLAUSIBLE SINK FOR AN EARLY DENSE CO_2 ATMOSPHERE? Stuart K. Stephens and David J. Stevenson, Division of Geological and Planetary Sciences, California Institute of Technology, Pasadena, California 91125.

Introduction: Importance of This Work

Many ideas about the early Martian climate involve the concept of a CO_2 atmosphere with a pressure of more than 1 bar in order to explain the presence of observed surface features (e.g., inferred high erosion rates, dendritic valley networks). One bar is about the atmospheric pressure on Earth now (only a very small fraction of which is CO_2). The present atmosphere on Mars is a mere seven thousandths of a bar. Carbonate formation would lower the CO_2 pressure and occurs easily in wet environments. This has been invoked to explain the destruction of a dense, early atmosphere on Mars. However, since surficial liquid water would only exist (in sufficient quantities) as long as the carbon dioxide pressure was above a level of about one atmosphere, an additional means is necessary to further reduce the pressure of the early atmosphere. To get it to the present pressure of 7 thousandths of a bar, we evaluate the concept of *dry* carbonate formation (i.e., without the presence of a liquid phase of water). Further, we point out the implications of such a process for the evolution of the atmospheric pressure over time (whether the transition from about 1 bar down to the present value may have been quick or gradual).

The Problem

The hypothesis that Mars once had a CO_2 atmosphere with a pressure much greater than today's value is not universally accepted because it rests on a chain of reasoning constrained mainly by images from orbiting spacecraft, and not by field observations. Spacecraft observations of dendritic valley networks, similar to water runoff channels on Earth, and previous high erosion rates inferred from the degradation of craters and other features, both indicate the possible long-term presence on the surface of substantial liquid water (transitory rivers at least, lakes or oceans perhaps), although other explanations for some of the observations have also been proposed. For liquid water to have existed at the surface over the millions of years thought to be necessary to explain the observations, the temperature most likely would have had to remain above the freezing point for that time. Given Mars' distance from the sun, such a surface temperature could only have been maintained if the atmosphere was dense enough that greenhouse conditions existed. Carbon dioxide is a good greenhouse gas and an early dense atmosphere in contact with abundant surface water would have permitted the formation of carbonates in sufficient quantities to reduce the atmospheric CO_2 pressure. However, there would have come a point as the temperature declined where the conditions would have been insufficient for further carbonate formation in this way. The lowest pressure at which wet carbonate formation continues would have been around 1 bar (corresponding to a greenhouse temperature about equal to the freezing point of water).

This work investigates an alternative sink for an early dense CO_2 atmosphere on Mars: dry carbonate formation — a process first proposed by Booth and Kieffer in 1978.

Questions Posed by Dry Carbonate

We are very interested in the decrease of atmospheric CO_2 pressure with time once the surface temperature drops below the freezing point. If, as we shall see, the carbonate produced on small silicate grains forms as submicron coatings through which further CO_2 penetration is progressively limited by diffusion, then the precise dependence of diffusivity on

temperature (itself decreasing with time) will determine whether the CO_2 pressure declines rapidly or slowly. It will also be of interest to determine whether dry carbonate formation should still be playing a role in further reducing the pressure below its present value.

A question which has been raised repeatedly in the past regarding carbonate formation on Mars — whether wet or dry — is: So, where is all this carbonate? Our calculations of the process and significance of dry carbonate formation will help answer this.

Booth and Kieffer's Experiment

In 1978, Booth and Kieffer examined carbonate growth within rock powders subjected to Mars-like environment simulations (including the near absence of liquid water). Their resulting yield was less than a monolayer of carbonate on about 40-micron grains in the span of several days. The authors show that this reaction rate more than accounts (by several orders of magnitude) for the destruction of 1 bar of CO_2 over geologic time (billions of years). However, their study had a major limitation, namely that there is no reliable basis for extrapolation, since less than a monolayer was formed, and the nature of the "rind" formed was not closely examined.

Present Theoretical Work

We attempted to find published results where the carbonate formed by CO_2 interaction with silicates in the absence of liquid water was actually examined (e.g., with a scanning electron microscope), but without success. In the absence of experimental results, we considered the worst case — that in which the formation of a rind limits the effectiveness of the rapid reaction reported by Booth and Kieffer. Namely, we considered the question: Is the process (of dry carbonate formation) reaction-limited or diffusion-limited? To get an idea of the actual diffusivity of CO_2 through carbonate, we extrapolated from experiments performed at high temperature to obtain an estimate of diffusion. We found that the actual diffusivity is *eighteen* orders of magnitude less than that for which the reaction rate limits the amount of carbonate produced. This implies a diffusion-limited reaction. Indeed, Booth and Kieffer's dry carbonate growth rate could be too large by about nine orders of magnitude, and this result would still old. In this sense, the reaction rate is irrelevant — it is the *diffusivity* that determines the rate of carbonate growth.

Over geologic time, this diffusion-limited dry carbonate formation is capable of forming a layer ~60 angstroms thick on silicate grains. For a 1-km regolith and 40-micron particles, this means that ~0.05 bar of CO_2 can be stored. This is a very conservative estimate, since we have probably underestimated the diffusivity and we have assumed that the rind is nonporous.

Discussion: Application and Relevance of This Work

We model the evolution of CO_2 pressure by realizing that we can obtain an estimate of diffusivity as a function of temperature from existing experimental data, and temperature as a function of CO_2 pressure from published greenhouse models. This relationship is constrained by the requirement that we get the right present pressure. Now, diffusivity is a very sensitive function of temperature and as T decreases to the present mean annual temperature, the diffusivity gets *much* smaller. The implication is that the current atmospheric pressure is decreasing slowly compared to its previous evolution. Detailed results will be presented at the conference.

Finally, in applying our results to current telescopic searches for carbonates on Mars, note that if the carbonate is indeed produced in thin (<<1-micron) layers, then it will not be

readily detectable in infrared observations. If carbonate is detected, as recently claimed, then it is ancient carbonate produced during epochs of liquid water on the surface.